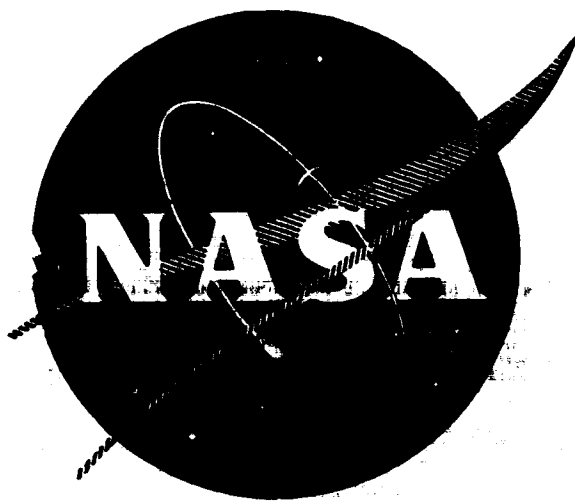


NASA-CR-72150

WANL-PR(EE)-003



Evaluation of Refractory/Austenitic Bimetal Combinations

Third Progress Report
by

R. W. Buckman, Jr. and R. C. Goodspeed

N67 18742

(ACCESSION NUMBER)	(THRU)
56	1
(PAGES)	(CODE)
NASA CR 72150	17
(NASA CR OR TMX OR AD NUMBER)	(CATEGORY)

FACILITY FORM 602

Prepared for
National Aeronautics and Space Administration
 Lewis Research Center
 Space Power Systems Division
 Under Contract NAS 3-7634



Astronuclear Laboratory
Westinghouse Electric Corporation

CFSTI PRICE(S) \$ _____

Hard copy (HC) 3.00

Microfiche (MF) 1.65

653 July 65

NOTICE

This report was prepared as an account of Government-sponsored work. Neither the United States nor the National Aeronautics and Space Administration (NASA), nor any person acting on behalf of NASA:

- A) Makes any warranty or representation, expressed or implied, with respect to the accuracy, completeness, or usefulness of the information contained in this report, or that the use of any information, apparatus, method, or process disclosed in this report may not infringe privately-owned rights; or
- B) Assumes any liabilities with respect to the use of, or for damages resulting from the use of any information, apparatus, method or process disclosed in this report.

As used above, "person acting on behalf of NASA" includes any employee or contractor of NASA, or employee of such contractor, to the extent that such employee or contractor of NASA or employee of such contractor prepares, disseminates, or provides access to, any information pursuant to his employment or contract with NASA, or his employment with such contractor.

Copies of this report can be obtained from:

National Aeronautics & Space Administration
Office of Scientific and Technical Information
Washington 25, D. C.
Attention: AFSS-A



Astronuclear
Laboratory
WANL-PR(EE)-003
NASA-CR-72150

EVALUATION OF REFRACTORY/AUSTENITIC BIMETAL COMBINATIONS

by

R. W. Buckman, Jr. and R. C. Goodspeed

Third Progress Report

Covering the Period

December 22, 1965 to June 22, 1966

Prepared for
NATIONAL AERONAUTICS AND SPACE ADMINISTRATION

Contract NAS 3-7634

Technical Management
P. L. Stone
NASA-Lewis Research Center
Space Power Systems Division

Westinghouse Astronuclear Laboratory
P. O. Box 10864
Pittsburgh, Pennsylvania 15236

EVALUATION OF REFRACTORY/AUSTENITIC BIMETAL COMBINATIONS

by

R. W. Buckman, Jr.

and

R. C. Goodspeed

ABSTRACT

Evaluation of the bond integrity of explosively bonded refractory/austenitic bimetal composites continued as five of the six diffusion annealing runs were completed. Inter-diffusion zone thicknesses of the annealed specimens, as determined metallographically, indicated that the composites could be grouped into three classes depending on the extent of reaction. Specimens of the nine previously selected combinations were thermally cycled. No indications of unbonding were observed. Room temperature tensile testing of specimens which were thermally exposed for 1600 hours at 1500°F indicated that the heat treatment resulted in appreciable decreases in strength and increases in elongation as compared to the as-bonded condition. Creep rupture testing of bimetal composites in the as-bonded condition was initiated.

TABLE OF CONTENTS

	<u>Page No.</u>
I. INTRODUCTION	1
II. PROGRAM STATUS	1
A. STARTING MATERIAL	1
B. DIFFUSION ANNEALING	2
C. THERMAL EXPOSURE	25
D. THERMAL CYCLING	28
E. CREEP RUPTURE	35
III. FUTURE WORK	38
IV. REFERENCES	39
APPENDIX I	40

LIST OF FIGURES

		<u>Page No.</u>
1.	Microstructures of Refractory Materials Used to Manufacture the Bimetal Composites	3
2.	Vycor Capsule Containing Ta Wrapped Bimetal Specimens After Annealing 1600 Hours at 1500°F	5
3.	Interdiffusion Zone Between Cb/321 Stainless Steel After Indicated Exposure	11
4.	Interdiffusion Zone Between Cb/347 Stainless Steel After Indicated Exposure	12
5.	Interdiffusion Zone Between Ta/321 Stainless Steel After Indicated Exposure	13
6.	Interdiffusion Zone Between Cb-1Zr/Inconel 600 After Indicated Exposure	14
7.	Average Interdiffusion Zone Thickness as Function of Time and Temperature for the three Classes of Austenitic/Refractory Bimetal Composites	16
8.	Interdiffusion Zone Thickness as a Function of Time and Temperature for Selected Austenitic/Refractory Bimetal Composites	17
9.	Interdiffusion Zone Thickness as a Function of Reciprocal Temperature	18
10.	The Parabolic Reaction Rate of Interdiffusion Zone Growth as a Function of Reciprocal Temperature	19
11.	Hardness Change in Refractory and Austenitic Components after Annealing for Specified Time	26
12.	Thermal Cycle Specimens and Restraint Fixture Prior to Assembly	29
13.	Thermal Cycling Test Rig	30
14.	Schematic View of Thermally Cycled Strip Showing Direction of Bow	31

LIST OF FIGURES (Continued)

	<u>Page No.</u>
15. Appearance of Indications of Bonded and Unbonded Bimetal Composites Using Pulse Echo Ultrasonic Technique	36
16. Creep and Creep Rupture Data for Austenitic Stainless Steel and Austenitic/Refractory Bimetal Composites at 1350°F	37

LIST OF TABLES

	<u>Page No.</u>
1. Mechanical Properties of Refractory Materials Used for Fabrication of Bimetal Composites	4
2. Delaminated Diffusion Annealed Refractory/Austenitic Bimetal Composites	6
3. Weight Loss Data for Diffusion Annealed Refractory/Austenitic Bimetal Composites	8
4. Interdiffusion Zone Thickness Data for Diffusion Annealed Refractory/Austenitic Bimetal Composites	9
5. Diffusion Annealed Refractory/Austenitic Bimetal Composite Specimens Tentatively Selected for Electron Beam Microprobe Analyses	21
6. Interdiffusion Zone Thickness and Knoop Hardness Traverse Data for Diffusion Annealed Refractory/Austenitic Bimetal Composites	22
7. Room Temperature Tensile Test Data on Refractory/Austenitic Bimetal Composites as-Bonded and After Thermal Exposure of 1600 Hours at 1500°F	27
8. Amount of Bow of Bimetal Composites Resulting from Thermal Cycling	32

LIST OF TABLES (Continued)

		<u>Page No.</u>
9.	Results of Dye Penetrant Inspection of As-Received Plus As-Thermally Cycled Composite Specimens	34
10.	1350°F Creep Rupture Properties of Refractory/Austenitic Bimetal Composites	35

I. INTRODUCTION

This is the third progress report covering the six month period from December 22, 1965 to June 22, 1966 under Contract NAS 3-7634, "Evaluation of Refractory/Austenitic Bimetal Combinations". The objective of this program is to evaluate the compatibility of various refractory/austenitic bimetal combinations after isothermal and cyclic thermal exposure. The refractory/austenitic bimetal composites were fabricated by explosive bonding.

During this period, evaluation of the bond integrity of the explosively bonded bimetal composites continued. Five of the six planned diffusion annealing runs were completed and each of the bimetal composites was placed into one of three classes according to the rate of growth of its interdiffusion zone. From these results nine diffusion specimens have been tentatively selected, subject to final NASA approval, for further evaluation by means of electron beam microprobe analyses. Specimens of the nine previously selected bimetal combinations were thermally cycled, while five of the nine specimens which had been thermally exposed (1600 hours at 1500^oF) were tensile tested. Creep rupture testing of bimetal composites in the as-bonded condition was also initiated.

II. PROGRAM STATUS

A. STARTING MATERIAL

During the report period, the bimetal composite originally identified as Cb-1Zr/321 stainless steel was found instead to be Cb-1Zr/Inconel 600. Identification was made by x-ray fluorescence, which indicated an approximate composition of 75%Ni, 15%Cr, 10%Fe, and no Ti. This analysis was performed when the microstructure of the austenitic component of the specimen that had been diffusion annealed for 1600 hours at 1400^oF appeared to more closely resemble Inconel 600 rather than 321 stainless steel. Soon afterwards, a piece of Cb-1Zr/321 stainless steel composite was obtained from NASA. This material was not received in time to conduct the full complement of tests. However, a thermal diffusion specimen and several 1" by 8" strips were included in the 1500^oF/1600 hour thermal exposure run, which is scheduled for completion during the month of August.

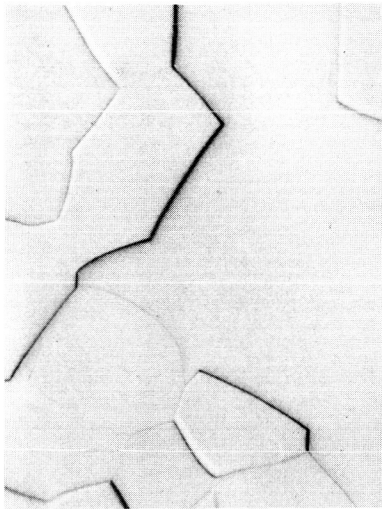
The microstructure, tensile properties, and hardness of the refractory materials (Cb, FS-85, Ta, and T-222) used in the fabrication of the bimetal composites were evaluated. The original Cb-1Zr material was not available for study. Figure 1 illustrates the microstructure of the four refractory materials, while mechanical property and hardness data are recorded in Table 1. All starting materials were recrystallized before explosive bonding with the exception of the tantalum which was stress relieved, which accounts for its comparatively high tensile strength and hardness and low ductility.

B. DIFFUSION ANNEALING

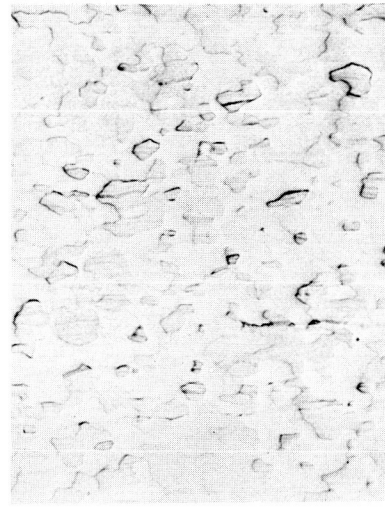
Five of the diffusion annealing treatments were completed. These anneals, accomplished in an ultra high vacuum of 10^{-8} torr maintained in all metal sealed, bakeable, sputter ion pumped systems, consisted of 1600 hours at 1400, 1500, and 1600°F and 2700 hours at 1400 and 1600°F. Approximately 2000 hours had been accumulated on the 2700 hour/1500°F run at the end of this report period. Figure 2 illustrates the typical appearance of a loaded capsule at the conclusion of a diffusion annealing run.

Apparent in Figure 2 is a black deposit on the inside surface of the Vycor tube. This type of deposit formed during all 5 anneals. Emission x-ray analyses of several of the deposits indicated that they consisted of Mn with a trace of Cr. No inward transfer of Si from the Vycor tube into the specimens annealed for 1600 hours at 1600°F was indicated by spectrographic analyses of successive layers of the Ta foil in which the specimens were wrapped.

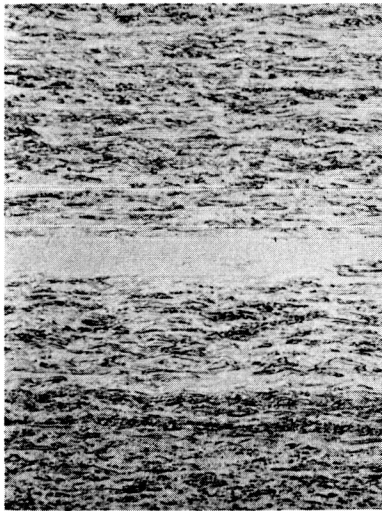
Each specimen from each run was carefully unwrapped and visually examined for indications of unbonding. A small number of specimens were delaminated when unwrapped or delaminated during handling. The combinations which delaminated during diffusion annealing are identified in Table 2. No inconsistencies occurred in as much as if a composite was delaminated after being annealed for a given time at a given temperature, it was also delaminated after being annealed for longer times at the same temperature as well as after annealing at higher temperatures.



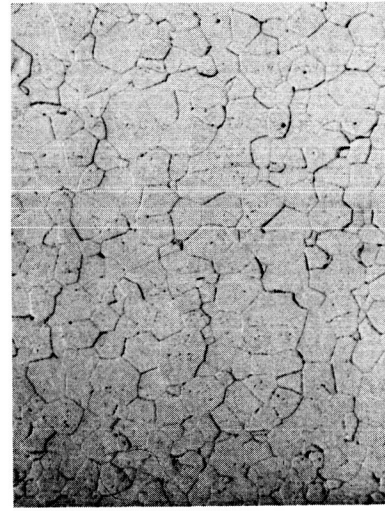
Cb



FS-85



Ta



T-222

FIGURE 1 - Microstructures of Refractory Materials Used to Manufacture
the Bimetal Composites 150X

**TABLE 1 - Mechanical Properties of Refractory Materials Used
for Fabrication of Bimetal Composites**

Composition	Yield Strength			UTS (psi)	Elongation (%)	Hardness DPH
	Upper (psi)	Lower (psi)	0.2% Offset (psi)			
Cb	---	---	13,100	24,900	44.5	73
FS-85	73,400	68,300	---	83,300	30.5	194
Ta ^(a)	---	---	64,900	73,900	14.0	159
T-222	---	---	81,600	106,400	28.5	238

(a) Ta sheet in the wrought plus stress relieved condition

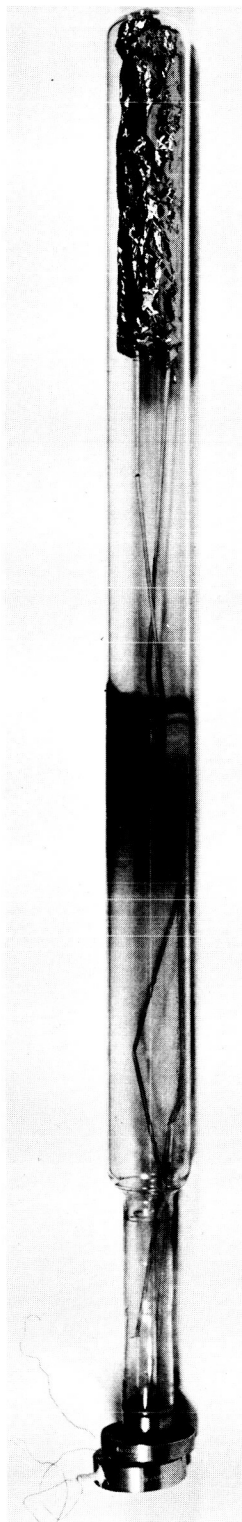


FIGURE 2 - Vycor Capsule Containing Ta Wrapped Bimetal Specimens After
Annealing 1600 Hours at 1500°F. Black Deposit Identified as Mn
is apparent on Upper End of Tube.

TABLE 2 - Delaminated Diffusion Annealed Refractory/Austenitic Bimetal Composites

Composition	Conditions Under Which Composites Delaminated ^a					
	1600 Hours at			2700 Hours at		
	1400°F	1500°F	1600°F	1400°F	1500°F ^b	1600°F
Ta/347	Not Del.(N.D.) ^d	Not Del.(0.15)	Del.	Not Del.(0.04)	---	Del.
FS-85/347	Not Del.(N.D.)	Not Del.(0.30)	Del.	Not Del.(0.08)	---	Del.
Ta/Inc. 600	Not Del.(0.45)	Del.	Del. ^d	Not Del.(0.70)	---	Del.
Ta/Hast. N	Del.	Del.	Del.	Del.	---	Del.

(a) Del. - Delaminated

(b) Not completed to date

(c) Numbers in parentheses are thicknesses of interdiffusion zones (in mils) in delaminated specimens. ND - None detected.

(d) Specimen delaminated along most of its length.

Each diffusion specimen was weighed after annealing and the weight change was determined. These data are recorded in Table 3 in the approximate order of decreasing weight loss. Many of the minor inconsistencies are probably due to relative position of the specimens within the various capsules. As expected from the composition of the deposits on the Vycor tubes, bimetal specimens containing 321 and 347 stainless steel (1.6 and 1.4% Mn respectively) exhibited greater weight losses than the bimetal combinations having Hastelloy N or Inconel 600 components (0.5 and 0.1% Mn respectively). However, the bimetal combinations containing either Hastelloy N or Inconel 600 exhibited a slight weight gain after the 1600 hour exposure at 1500°F. The pressure during the exposure never went below 2×10^{-8} torr and was approximately a decade higher than observed on the other diffusion runs. Therefore it is possible that a slight leak may have developed during the test and thus the refractory metal portion of the bimetal specimens could have been contaminated. Sections of several of the specimens from this run are being analyzed for oxygen to determine the extent of any contamination.

Each specimen was then metallographically examined to determine the effects of time at temperature on the interface between the refractory and austenitic components. The metallographic procedures and etchants are listed in Appendix I. Interface zone thicknesses were measured from 400X photomicrographs and are listed in Table 4. Where ranges of interface zone thickness are given in the table, systematic variation of thickness occurred with position along the length of the bond interface (see Figure 3). The bimetal composites can be conveniently separated into three classes based on the interdiffusion zone thickness. Class I is comprised of bimetal composites containing Ta or T-222 and 321 or 347 stainless steels. These composites have the lowest rate of interdiffusion zone growth. Class III is entirely comprised of combinations having either Inconel 600 or Hastalloy N as their austenitic component and represents the fastest rate of zone growth. Included in this class are Cb/Inconel 600, Ta/Inconel 600, FS-85/Inconel 600, Cb-1Zr/Inconel 600, and FS-85/Hastalloy N. Those combinations having an intermediate rate of zone growth were grouped together into Class II. This class contains those combinations having Cb or a Cb alloy and 321 or 347 stainless steels and the T-222/Inconel 600 combination.

TABLE 3 - Weight Loss Data for Diffusion Annealed Refractory/Austenitic Bimetal Composites

Composition	Weight Loss (Percent)					
	1600 Hours			2700 Hours		
	1400°F	1500°F	1600°F	1400°F	1500°F	1600°F
FS-85/347	.014	.030	.094	.015	(b)	.088
Cb-1Zr/347	.011	.027	.068	.017	---	.087
Cb/347	.008	.025	.051	.020	---	.079
Cb/321	.014	.023	.050	.009	---	.072
FS-85/321	.006	.053	.048	.013	---	.067
Ta/347	.013	.022	.036	.013	---	.063
T-222/347	.006	.020	.041	.012	---	.055
Ta/321	.007	.019	.033	.011	---	.053
T-222/321	.009	.020	.031	.015	---	.050
Ta/Hast. N	.007	(.001 ^a)	.038	.008	---	.030
FS-85/Inc. 600	.002	(.012 ^a)	.025	.004	---	.019
FS-85/Hast. N	.006	(.007 ^a)	.027	.004	---	.016
Cb/Inc. 600	.002	(.006 ^a)	.028	.009	---	.015
Ta/Inc. 600	.012	(.009 ^a)	.025	.006	---	.017
T-222/Inc. 600	.005	(.002 ^a)	.023	.005	---	.016
Cb-1Zr/Inc. 600	.004	(.023 ^a)	.026	.005	---	.012

(a) Data represents weight gain.

(b) Test in progress.

NOTE: All specimens were 1/4" w x 1" l x 0.09" t

TABLE 4 - Interdiffusion Zone Thickness⁽¹⁾ Data for Diffusion Annealed Refractory/Austenitic Bimetal Composites*

Composition	Zone Thickness (In Mils)					
	1600 Hours At:		2700 Hours At:		1600°F	
	1400°F	1500°F	1400°F	1500°F(2)	1400°F	1600°F
Class I						
1. T-222/321	a	0.20	0.15	---	---	0.15
2. T-222/347	a	0.15	0.30	---	---	0.30
3. Ta/321	a	0.25	0.30	---	---	0.63
4. Ta/347	a	0.15	b	---	---	b
Range	---	0.15-0.25	0.15-0.30	---	---	0.15-0.63
Average	a	0.19	0.25	---	---	0.36
Class II						
1. Cb/321	0.17	0.31-0.70	1.20	---	0.16-0.31	1.55
2. Cb/347	0.17	0.30	1.00	---	0.12-0.23	1.25
3. Cb-1Zr/347	a	0.15	1.20	---	a	1.33
4. FS-85/321	a	0.55	0.75	---	0.08	1.40
5. FS-85/347	a	0.30	b	---	0.08	b
6. T-222/Inc. 600	c	0.65	1.30	---	0.12	1.33
Range	a-0.17	0.15-0.70	0.75-1.30	---	a-0.31	1.25-1.55
Average	0.06	0.41	1.10	---	0.11	1.37
Class III						
1. Cb/Inc. 600	0.60	0.20	1.60	---	0.86	1.87
2. Ta/Inc. 600	0.45	0.00	b	---	0.70	b
3. FS/Inc. 600	0.50	0.35	2.00	---	0.63	2.50
4. Cb-1Zr/Inc. 600	0.50	0.15	1.80	---	0.78	2.20
5. FS-85/Hast. N	0.45	0.50d	1.30	---	0.55	2.03
Range	0.45-0.60	1.00-1.35	1.30-2.00	---	0.55-0.86	1.87-2.50
Average	0.50	1.17	1.67	---	0.70	2.15

a - None detected
b - Specimen delaminated prior to mounting
c - Interdiffusion zone present, not well enough defined to measure.
d. Data point excluded from range and average.
(1) Determined Metallographically
(2) Not completed to date

Photomicrographs of the interdiffusion zones as a function of time and temperature are shown for Cb/321 and Cb/347 (Class II), Ta/321 (Class I), and Cb-1Zr/Inconel 600 (Class III), in Figures 3 through 6 respectively. Only the austenitic component of each specimen is etched, because the etch polishing procedure used for the refractory materials severely attacks the austenitic component and much of the interdiffusion zone.

It is evident from the photomicrographs that the make-up of some of the zones is quite complex. Occasionally they are composed of two or more phases, some of which may have precipitated out during cooling from the diffusion annealing temperature. No attempt has been made to identify these phases, although they are undoubtedly similar to those reported by Manzione et al, for a Cb-1Zr/316 stainless steel couple⁽¹⁾, by Goldschmidt for a Fe/Cb couple⁽²⁾, and by Birks and Seebold for a Cb/stainless steel couple⁽³⁾. Such an analysis will be made at a later date on nine selected specimens which will be studied by means of an electron beam microprobe analyzer. The position of the original boundaries within the interdiffusion zone widths is not precisely known. However, voids, when present, are always within the austenitic material. Thus there appears to be a net diffusion of Ni, Cr, and Fe into the refractory material.

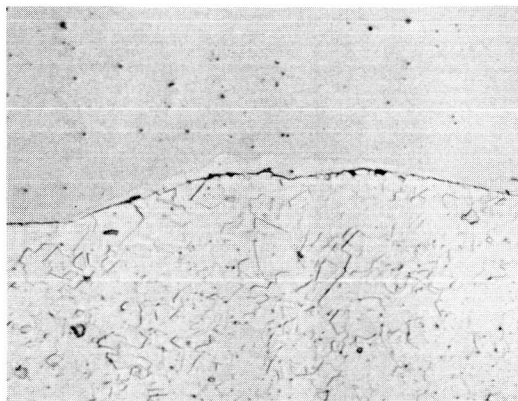
According to classical diffusion theory, the depth of diffusion (X) is proportional to the square root of both time (t) and diffusivity (D)

$$X \propto \sqrt{Dt}$$

and the log of diffusivity is proportional to the reciprocal of temperature (1/T)

$$\log D \propto 1/T.$$

Thus plots of X versus \sqrt{t} should result in straight lines which pass through the origin. The slopes of these lines should be proportional to \sqrt{D} . Plots of $\log(X^2)$ versus 1/T should also be straight lines.

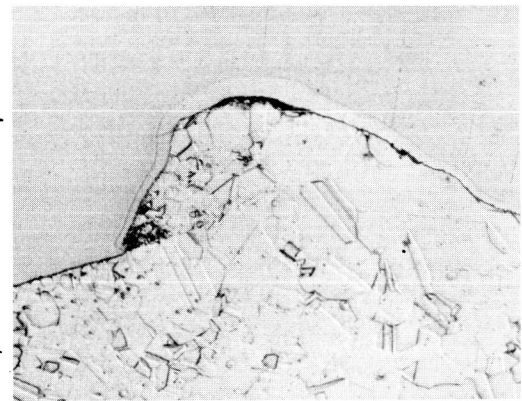


1400°F

1600 Hrs.

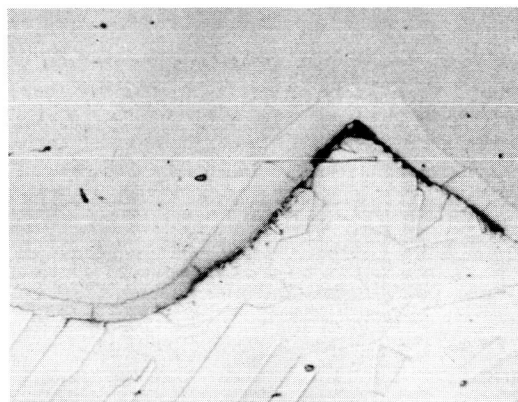
← Cb →

← 321 →



1400°F

2700 Hrs.



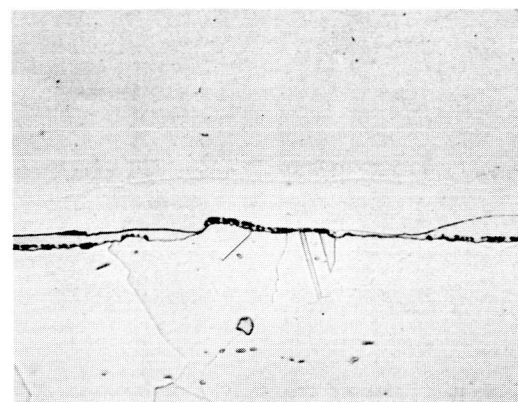
1500°F

1600 Hrs.

← Cb →

← 321 →

CLASS II

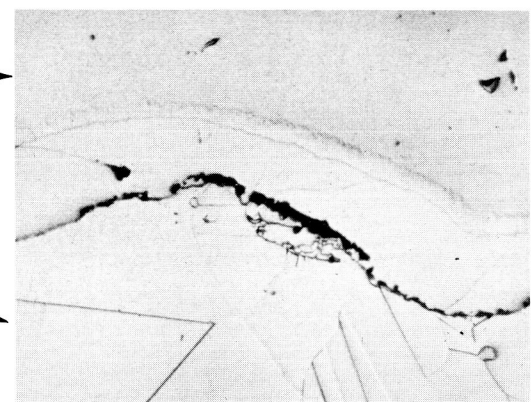


1600°F

1600 Hrs.

← Cb →

← 321 →



1600°F

2700 Hrs.

FIGURE 3 - Interdiffusion Zone Between Cb/321 Stainless Steel
(Class II Bimetal) After Indicated Exposure 400X

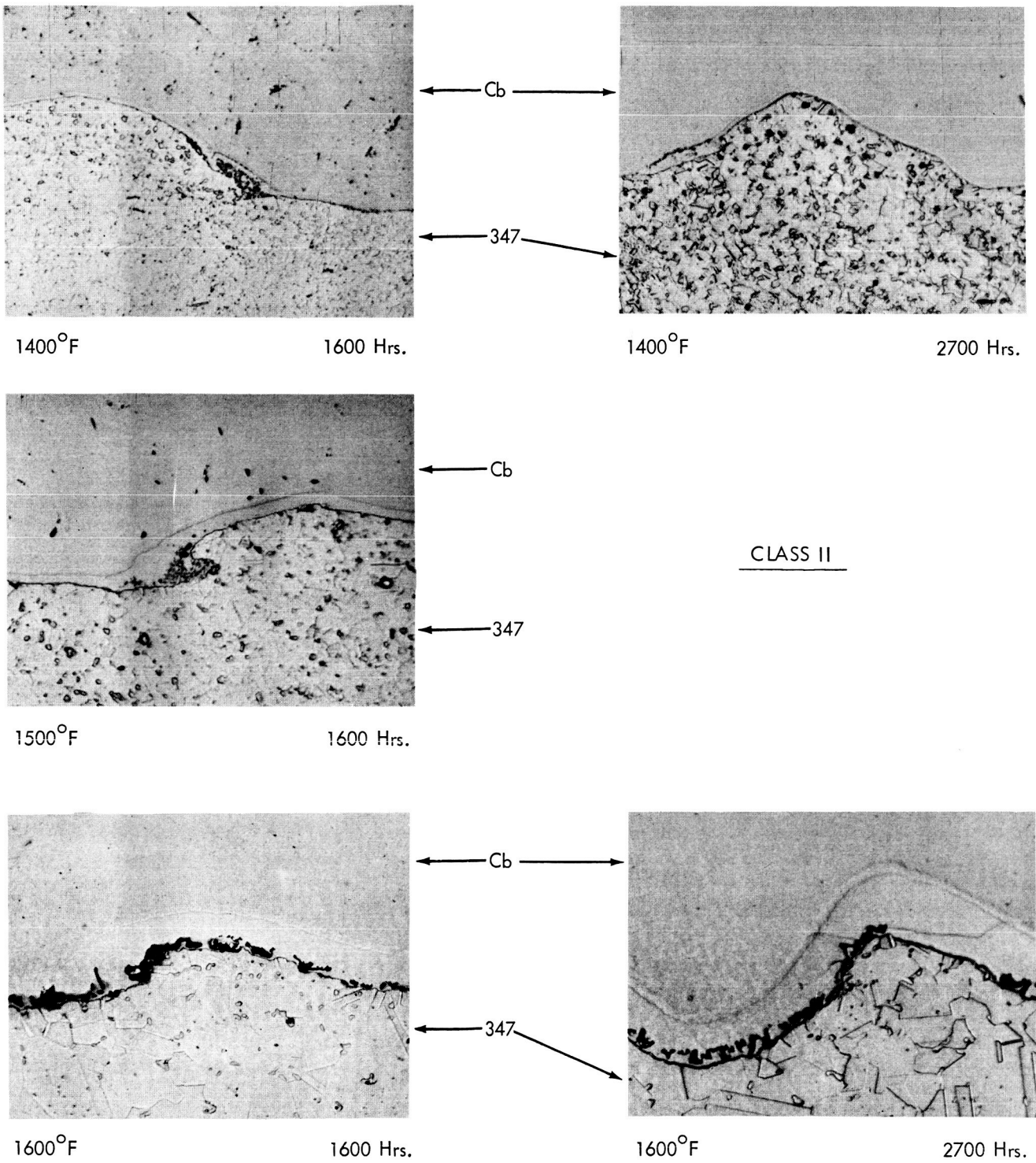


FIGURE 4 - Interdiffusion Zone Between Cb/347 Stainless Steel
(Class II Bimetal) After Indicated Exposure 400X

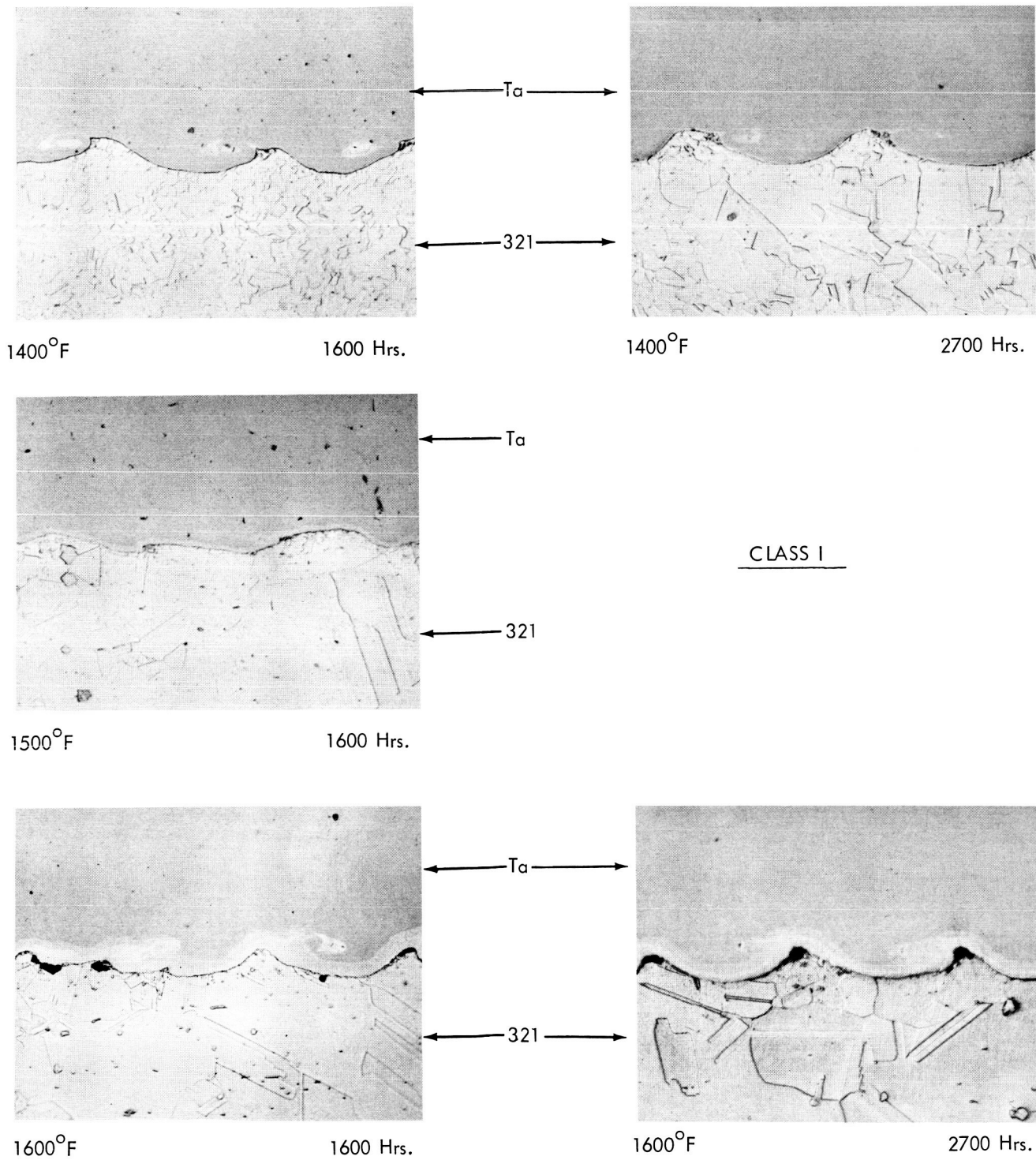


FIGURE 5 - Interdiffusion Zone Between Ta/321 Stainless Steel
(Class I Bimetal) After Indicated Exposure 400X

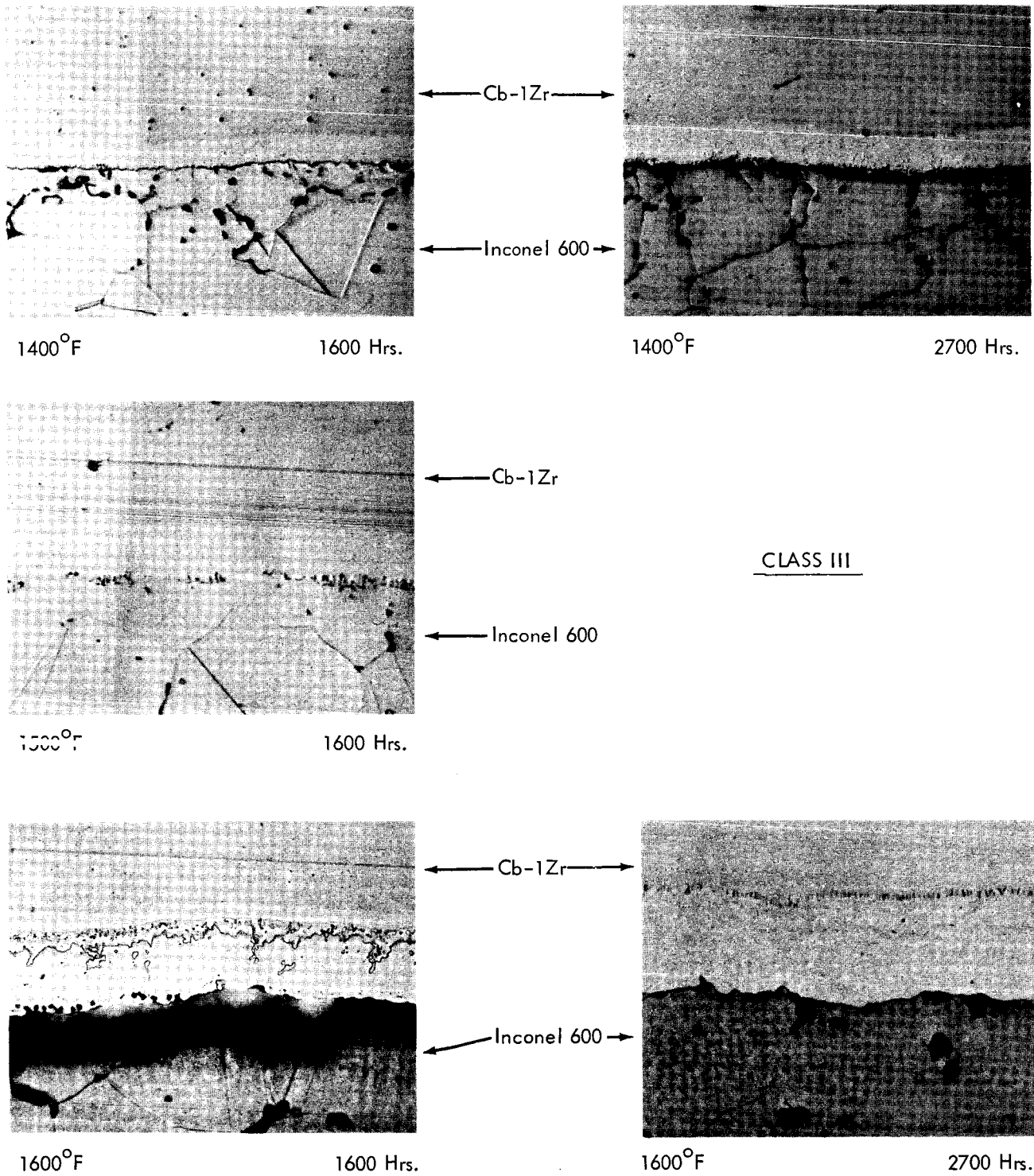


FIGURE 6 - Interdiffusion Zone Between Cb-1Zr/Inconel 600
(Class III Bimetal) After Indicated Exposure 400X

While the measured thicknesses represent metallographically observable interdiffusion zone thicknesses, rather than true diffusion depths, the metallographic data will be analytically treated according to diffusion theory. Interdiffusion zone thickness is plotted as a function of the square root of time for each annealing temperature in Figures 7 and 8. In Figure 7 the average thickness for each of the three classes of compositions is plotted for temperatures of 1400 and 1600°F. Ranges of thickness are also included. As can be seen, the data can be plotted as straight lines passing through the origin, as predicted. At 1400°F, the extent of reaction of Classes I and II are quite similar. However, at 1600°F, the extent of reaction of Class II is considerably greater than that of Class I. Figure 8 shows the data again for the 1400 and 1600°F diffusion anneals, for a number of actual bimetal combinations representing all three classes. As in the previous figure, the limited number of data points are reasonably approximated by straight lines passing through the origin. One consequence of this relationship is that for any given composite combination the zone thickness formed after 2700 hours at a given temperature is only about 30% greater than that formed after 1600 hours at the same temperature. This minor difference is well illustrated in Figures 3 through 6.

The square of the zone thickness (X) is plotted in Figure 9 as a function of $1/T$ for combinations representative of the three classes. Data for the Cb-1Zr/Inconel 600 is described reasonably well by a straight line but the slope of the line definitely changes for the Ta/321 as the annealing temperature was lowered from 1500°F to 1400°F. This change in slope, indicative of a change in diffusion mechanism is also shown in Figure 10, where the parabolic reaction rate $K(\frac{\partial X}{\partial t^{1/2}})^*$ is plotted as a function of $1/T$.

The rate of growth of the interdiffusion zone between the austenitic and refractory bimetal composites is assumed to obey the Arrhenius rate equation $K = Ae^{-Q/RT}$ where K is the parabolic rate of zone growth, in-hr^{-1/2}; A is a constant; Q is an activation energy cal/mol; R is the appropriate gas constant and T is the temperature in °K. The rate of zone growth for the bimetal couples Cb/321, Ta/321, T-222/347, and Cb/Inconel 600 is plotted as a function

* X is zone thickness and t is time in hours.

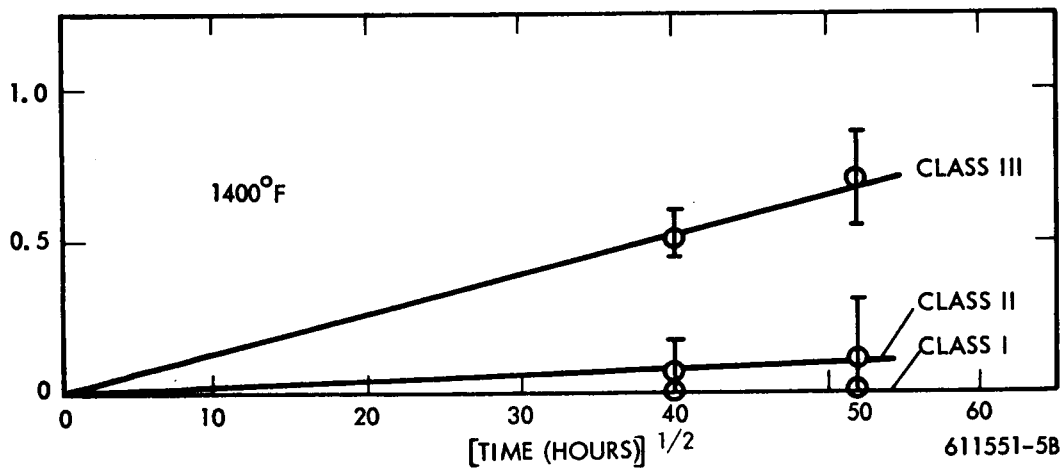
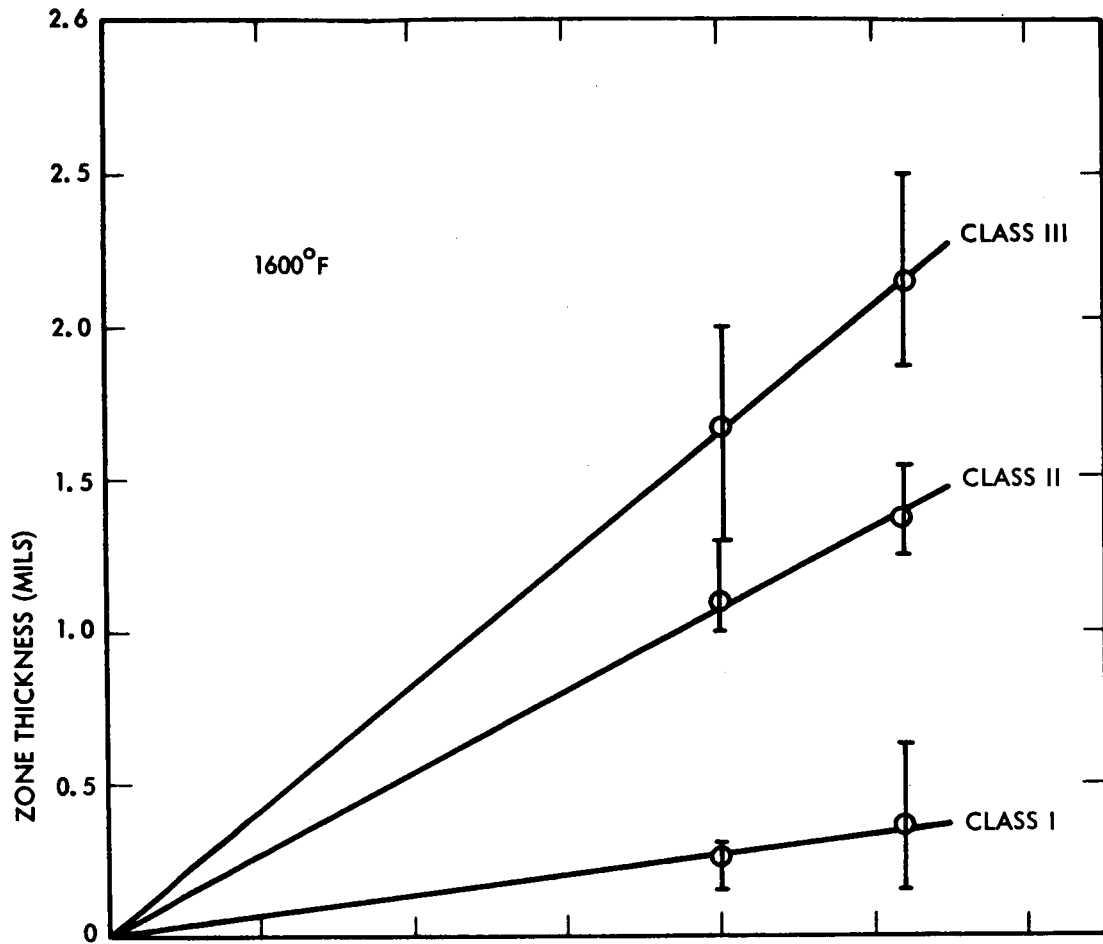


FIGURE 7 - Average Interdiffusion Zone Thickness as Function of Time and Temperature for the three Classes of Austenitic/Refractory Bimetal Composites

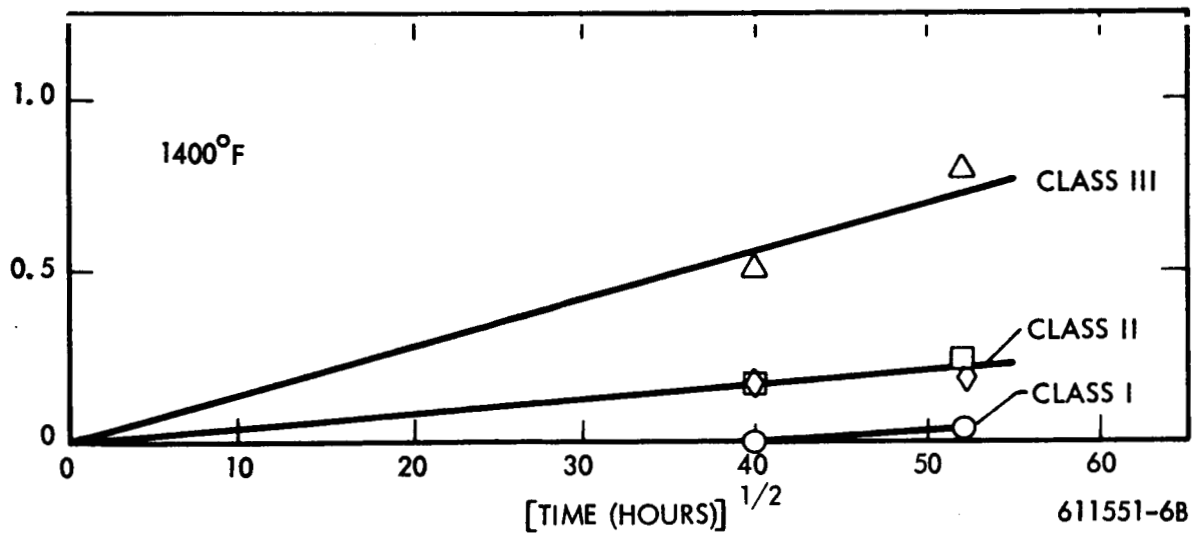
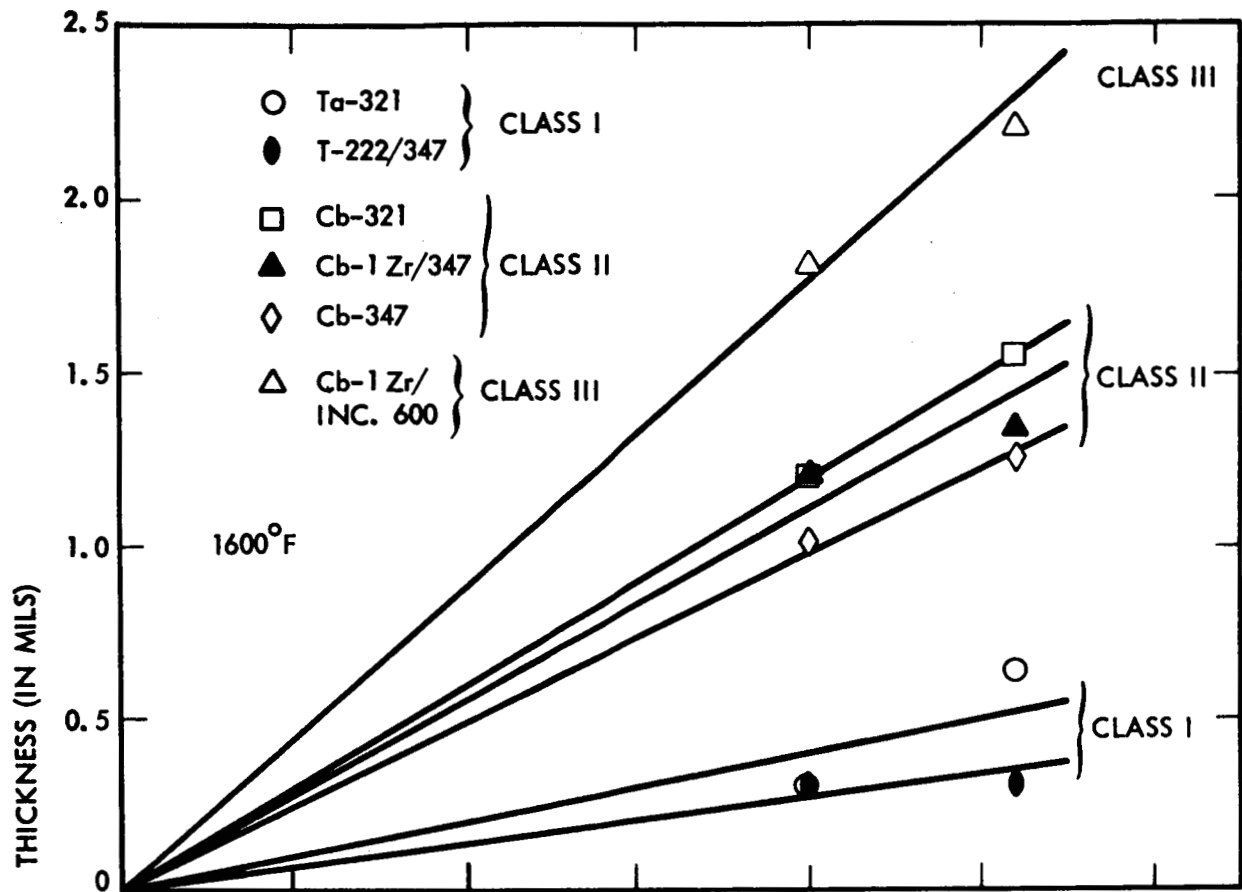


FIGURE 8 - Interdiffusion Zone Thickness as a Function of Time and Temperature for Selected Austenitic/Refractory Bimetal Composites

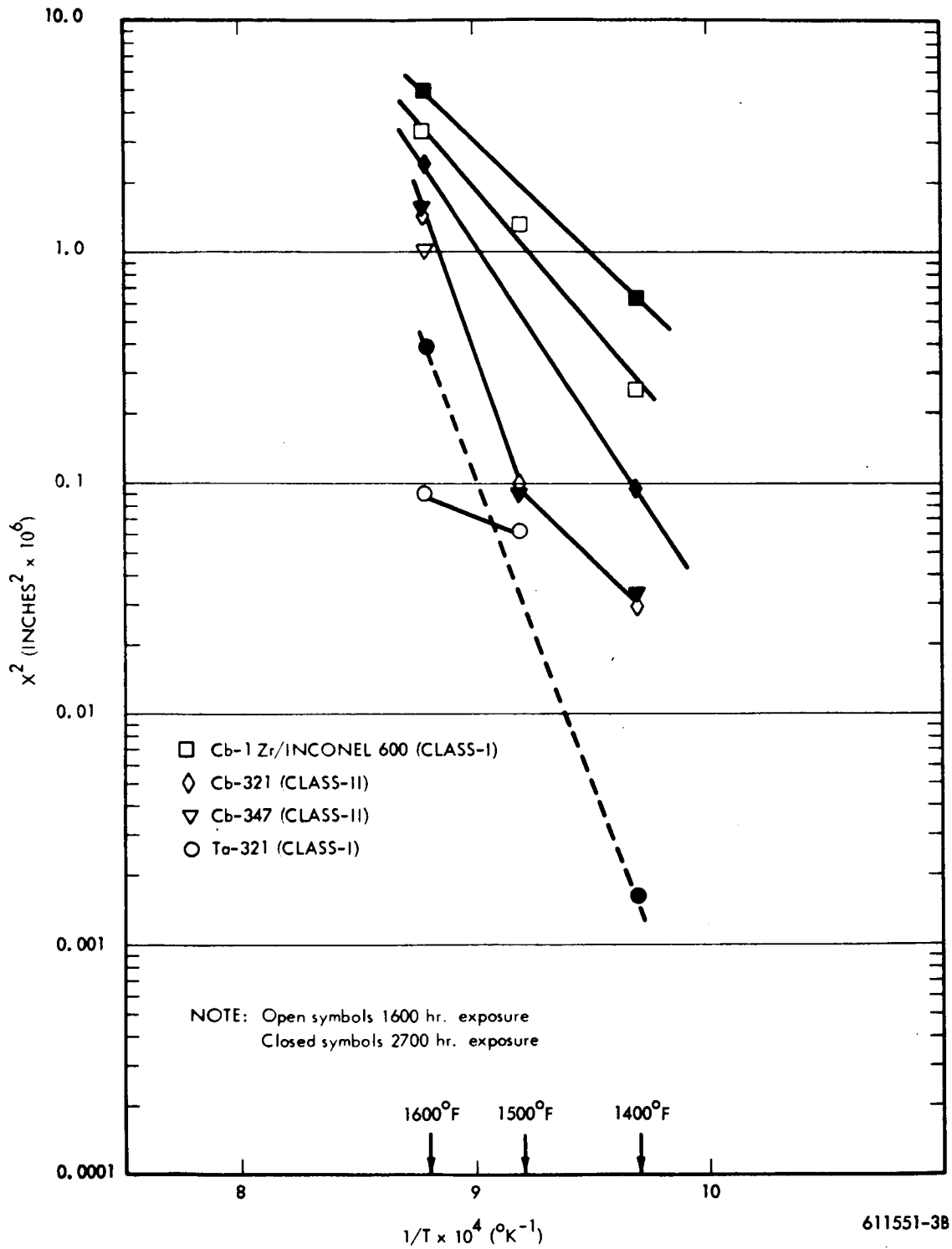


FIGURE 9 - Interdiffusion Zone Thickness as a Function of Reciprocal Temperature

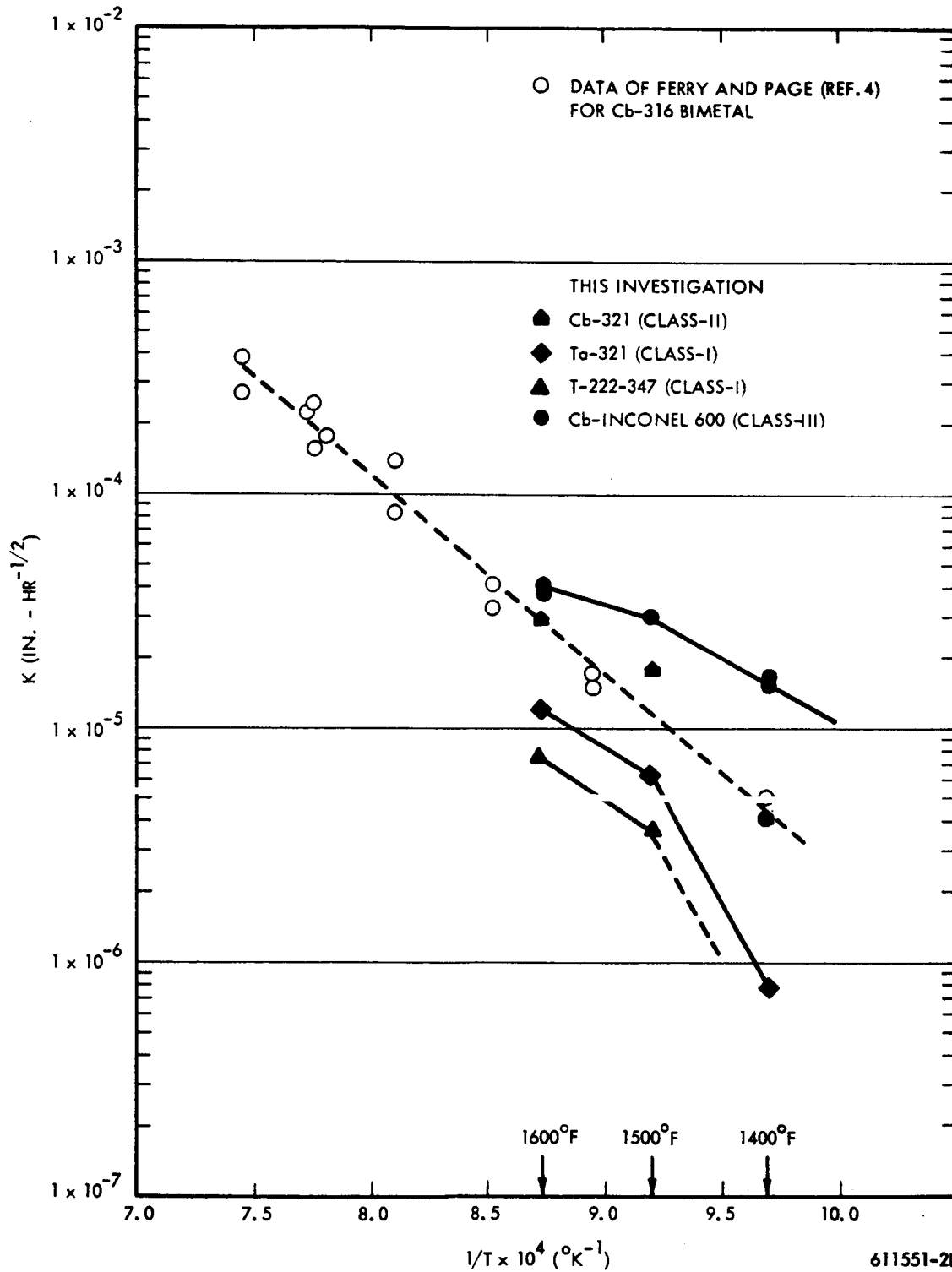


FIGURE 10 - The Parabolic Reaction Rate of Interdiffusion Zone Growth as a Function of Reciprocal Temperature

of the inverse temperature in Figure 10. Also on Figure 10 is plotted the zone growth data of Ferry and Page⁽⁴⁾ for 316-Cb determined for short times at higher temperatures. The rate of zone growth for the Cb-321 and Cb-347 were essentially identical for the experimental conditions investigated and agree very well with the data of Ferry and Page⁽⁴⁾ indicating the mechanism of interdiffusion between Cb and these three types of stainless steels is very similar. However, the rate of interdiffusion between Ta and the stabilized stainless steels was significantly less than for the columbium and as the annealing temperature was lowered to 1400°F, the difference was greater. T-222, which contains hafnium, exhibited a lower rate of interdiffusion than the pure tantalum as no reaction zone was observed metallographically at 400X after annealing 2700 hours at 1400°F. At 1600°F, the rate of zone growth between T-222 and the stainless steel was essentially the same as that between Cb and 321 at 1450°F. Substitution of Inconel 600 or Hastelloy N for the austenitic material resulted in a higher rate of interdiffusion irrespective of the refractory metal component. From compositional considerations, it appears that the nickel content may be the constituent which is exerting the greatest influence in the diffusion kinetics (Inconel 600 and Hastelloy N contain 75% Ni vs. 10% Ni for the 321 and 347 stainless steels). Electron microscopy techniques will be used to examine the interdiffusion zone in conjunction with the electron microprobe analysis which will be performed on selected specimens. The list of the specimens selected subject to final NASA approval, is listed in Table 5. Each of the three classes is represented in this selection.

Microhardness traverses were taken on each of the diffusion annealed bimetal composite specimens at distances of 1,2,3,5,10, and 20 mils from the interface into both the refractory and austenitic stainless steel components. Where interdiffusion zones were present, the measurements were taken at the same increments from the zone interfaces as observed metallographically since the location of the original interface could not be precisely ascertained. These data are presented in Table 6 along with the hardness data previously obtained on the as-received composites. The changes in hardness for a particular composite represent the net effect of a number of phenomena, which include thermal recovery during annealing, grain size effects, and chemical concentration changes due to diffusion. A

**TABLE 5 - Diffusion Annealed Refractory/Austenitic Bimetal Composite Specimens
Tentatively Selected for Electron Beam Microprobe Analyses**

Class	Composition	Annealing Temperature (°F)	Annealing Time (hrs.)	Interdiffusion Zone Thickness (mils)
I	Ta/321	1500	1600	0.25
		1600	1600	0.30
		1600	2700	0.63
	T-222/347	1600	1600	0.30
		1600	2700	0.30
	II	Cb/321	1500	1600
Cb/347		1500	1600	0.30
Cb-1Zr/347		1600	1600	1.20
III	Cb-1Zr/Inc. 600	1500	1600	1.15

TABLE 6 - Interdiffusion Zone Thickness and Knoop Hardness Traverse Data for Diffusion Annealed Refractory/Austenitic Bimetal Composites

Class and Composition	Condition	Idf. Zone Thickness (mils)	Knoop Hardness												
			Distance from Interface (mils)												
			Refractory Material						Austenitic Material						
			20	10	5	3	2	1	1	2	3	5	10	20	
Class I T-222/321	As Bonded	---	310	351	351	385	381	390	468	447	387	409	324	274	
	1400°F/1600 Hrs.	a	332	322	330	340	382	424	245	242	226	215	209	204	
	1500°F/1600 Hrs.	0.20	374	385	407	417	430	438	235	227	234	221	227	206	
	1600°F/1600 Hrs.	0.15	332	374	361	417	420	367	189	201	195	163	174	173	
	1400°F/2700 Hrs.	a	289	313	342	348	361	381	241	236	230	254	212	233	
	1500°F/2700 Hrs.	---													
	1600°F/2700 Hrs.	0.15	345	368	390	409	443	468	201	194	178	152	135	153	
	T-222/347	As Bonded	---	335	355	394	413	385	378	488	417	447	458	355	303
		1400°F/1600 Hrs.	a	319	349	324	346	377	349	203	212	218	196	189	182
		1500°F/1600 Hrs.	0.15	368	307	425	400	475	434	184	219	204	215	212	190
		1600°F/1600 Hrs.	0.30	322	371	407	435	451	451	156	171	166	161	169	163
		1400°F/2700 Hrs.	a	326	335	351	342	351	345	259	219	205	209	176	219
1500°F/2700 Hrs.		---													
Ta/321	1600°F/2700 Hrs.	0.30	315	378	425	413	409	374	129	159	151	164	150	150	
	As Bonded	---	171	189	207	207	207	201	473	473	443	405	368	326	
	1400°F/1600 Hrs.	a	154	163	171	184	180	186	188	186	196	178	168	160	
	1500°F/1600 Hrs.	0.25	186	173	176	180	191	185	173	174	186	178	177	176	
	1600°F/1600 Hrs.	0.30	128	164	165	167	173	163	167	181	173	156	143	140	
	1400°F/2700 Hrs.	0.04	155	167	166	176	172	175	187	185	186	185	175	167	
Ta/347	1500°F/2700 Hrs.	---													
	1600°F/2700 Hrs.	0.63	162	162	168	157	168	143	155	182	145	127	138	134	
	As Bonded	---													
	1400°F/1600 Hrs.	a	168	171	160	165	181	169	212	209	218	190	216	181	
	1500°F/1600 Hrs.	0.15	170	183	206	192	200	189	186	217	221	207	202	205	
	1600°F/1600 Hrs.	b													
Class II Cb/321	1400°F/2700 Hrs.	0.04	167	157	164	172	177	179	217	212	217	205	213	197	
	1500°F/2700 Hrs.	---													
	1600°F/2700 Hrs.	b													
	As Bonded	---	108	125	116	128	133	138	421	398	381	409	305	293	
	1400°F/1600 Hrs.	0.17	83	96	97	106	111	108	171	171	174	166	165	161	
	1500°F/1600 Hrs.	0.31-0.70	65	98	107	120	107	106	135	164	169	156	164	150	
1600°F/1600 Hrs.	1.20	90	110	109	116	136	92	145	153	155	151	151	125		
1400°F/2700 Hrs.	0.16-0.31	80	93	92	96	98	96	177	167	180	173	191	165		
1500°F/2700 Hrs.	---														
1600°F/2700 Hrs.	1.55	81	88	106	104	105	98	119	133	133	132	144	131		

TABLE 6 - Interdiffusion Zone Thickness and Knoop Hardness Traverse Data for Diffusion Annealed Refractory/Austenitic Bimetal Composites (Continued)

Class and Composition	Condition	Idf. Zone Thickness (mils)	Knoop Hardness											
			Distance from Interface (mils)											
			Refractory Material						Austenitic Material					
			20	10	5	3	2	1	1	2	3	5	10	20
Cb/347	As Bonded	---	107	119	127	121	120	118	434	458	430	394	336	315
	1400°F/1600 Hrs.	0.17	77	87	88	103	105	110	225	222	229	207	195	180
	1500°F/1600 Hrs.	0.30	97	107	114	107	112	117	191	206	205	224	217	224
	1600°F/1600 Hrs.	1.00	80	89	109	118	124	113	159	162	169	150	166	150
	1400°F/2700 Hrs.	0.12-0.23	87	95	113	112	115	113	201	204	206	210	196	186
	1500°F/2700 Hrs.	---												
Cb-1Zr/347	As Bonded	---	150	171	167	171	174	168	463	409	409	425	364	313
	1400°F/1600 Hrs.	a	123	126	153	167	171	175	219	222	229	208	196	189
	1500°F/1600 Hrs.	0.15	133	149	169	200	202	219	195	214	222	215	191	194
	1600°F/1600 Hrs.	1.20	102	126	156	190	203	211	145	191	184	188	176	166
	1400°F/2700 Hrs.	a	125	126	153	167	169	180	219	217	219	205	217	177
	1500°F/2700 Hrs.	---												
FS-85/321	As Bonded	---	267	303	282	285	218	265	430	405	390	390	303	318
	1400°F/1600 Hrs.	a	232	238	266	295	292	301	178	191	192	175	165	161
	1500°F/1600 Hrs.	0.55	240	247	294	347	353	344	156	176	200	171	166	179
	1600°F/1600 Hrs.	0.75	222	336	295	354	356	341	117	136	158	147	132	147
	1400°F/2700 Hrs.	0.08	236	229	259	274	278	267	177	178	180	166	162	153
	1500°F/2700 Hrs.	---												
FS-85/347	As Bonded	---	298	293	305	271	308	326	413	390	329	329	271	271
	1400°F/1600 Hrs.	a	256	257	286	300	310	290	228	233	233	213	177	177
	1500°F/1600 Hrs.	0.30	262	264	272	385	388	329	196	204	205	214	198	195
	1600°F/1600 Hrs.	b												
	1400°F/2700 Hrs.	0.08	236	241	278	282	285	276	189	205	212	182	189	173
	1500°F/2700 Hrs.	---												
T-222/Inc. 600	As Bonded	---	295	313	374	358	398	358	430	409	374	342	321	278
	1400°F/1600 Hrs.	c	295	334	361	344	353	382	178	185	180	169	152	197
	1500°F/1600 Hrs.	0.65	309	338	341	403	421	388	188	190	177	169	169	186
	1600°F/1600 Hrs.	1.30	312	330	361	374	394	394	134	161	167	166	180	179
	1400°F/2700 Hrs.	0.12	305	336	336	361	390	364	192	186	174	155	175	188
	1500°F/2700 Hrs.	---												
	1600°F/2700 Hrs.	1.33	305	335	326	378	355	378	140	143	157	157	164	176

TABLE 6 - Interdiffusion Zone Thickness and Knoop Hardness Traverse Data for Diffusion Annealed Refractory/Austenitic Bimetal Composites (Continued)

Composition	Condition	Idf. Zone Thickness (mils)	Knoop Hardness												
			Distance from Interface (mils)												
			Refractory Material						Austenitic Material						
			20	10	5	3	2	1	1	2	3	5	10	20	
Class III Cb/Inc. 600	As Bonded	---	112	118	112	119	129	126	374	300	295	313	295	236	
	1400°F/1600 Hrs.	0.60	93	83	98	105	108	109	154	176	207	165	151	161	
	1500°F/1600 Hrs.	1.20	92	98	111	109	97	91	164	158	159	208	200	165	
	1600°F/1600 Hrs.	1.60	73	86	102	98	101	92	159	189	201	178	161	156	
	1400°F/2700 Hrs.	0.86	78	81	94	82	77	76	111	136	144	153	149	145	
	1500°F/2700 Hrs.	---													
	1600°F/2700 Hrs.	1.87	75	83	100	100	80	81	168	124	166	154	151	167	
Ta/Inc. 600	As Bonded	---	188	183	180	191	193	216	378	351	358	351	318	247	
	1400°F/1600 Hrs.	0.45	175	165	170	167	178	179	157	186	180	160	174	170	
	1500°F/1600 Hrs.	1.00	197	182	189	191	171	185	128	189	197	166	175	200	
	1600°F/1600 Hrs.	b													
	1400°F/2700 Hrs.	0.70	130	143	128	153	160	153	164	171	155	152	132	139	
	1500°F/2700 Hrs.	---													
	1600°F/2700 Hrs.	b													
FS-85/Inc. 600	As Bonded	---	278	336	269	289	310	298	413	409	451	355	358	267	
	1400°F/1600 Hrs.	0.50	256	238	268	271	282	282	172	191	192	165	171	161	
	1500°F/1600 Hrs.	1.35	250	258	270	301	294	353	183	169	174	175	176	170	
	1600°F/1600 Hrs.	2.00	227	221	245	295	286	275	174	160	162	166	188	180	
	1400°F/2700 Hrs.	0.63	231	241	247	269	265	267	145	192	184	179	169	153	
	1500°F/2700 Hrs.	---													
	1600°F/2700 Hrs.	2.50	225	236	225	225	236	225	176	170	178	176	161	157	
Cb-1Zr/Inc. 600	As Bonded	---	142	152	148	153	164	154	398	390	381	364	295	292	
	1400°F/1600 Hrs.	0.50	127	135	153	156	165	157	149	164	171	159	152	165	
	1500°F/1600 Hrs.	1.15	138	153	162	168	173	149	206	217	175	178	170	175	
	1600°F/1600 Hrs.	1.80	101	111	107	133	119	112	138	166	169	170	154	170	
	1400°F/2700 Hrs.	0.78	137	123	161	155	158	158	144	157	164	185	157	168	
	1500°F/2700 Hrs.	---													
	1600°F/2700 Hrs.	2.20	114	112	133	93	114	120	171	146	148	178	155	158	
FS-85/Hast. N	As Bonded	---	241	271	280	293	313	323	451	390	390	390	326	287	
	1400°F/1600 Hrs.	0.45	236	256	246	282	280	308	178	176	195	178	173	195	
	1500°F/1600 Hrs.	0.50	262	266	258	278	285	292	212	214	190	201	197	202	
	1600°F/1600 Hrs.	1.30	207	219	258	292	302	322	127	158	175	169	153	189	
	1400°F/2700 Hrs.	0.55	245	254	278	278	274	305	141	184	133	161	174	186	
	1500°F/2700 Hrs.	---													
	1600°F/2700 Hrs.	2.03	193	225	221	212	186	237	140	145	172	151	162	144	

NOTES: (a) None detected
(b) Delaminated during exposure

detailed interpretation of this data will not be attempted until electron microprobe results become available. However, it was generally observed that the bulk hardness* of the austenitic material was essentially recovered after the 1600 hours at 1400°F and little change was observed after heating for longer times or at higher temperatures (see Figure 11). The hardness of the columbium and tantalum was not raised significantly during the explosive bonding process and this increment of hardness increase was recovered in the columbium after 2700 hours at 1400°F and 1600 hours at 1600°F. Since the tantalum was explosive bonded in the as-worked and stress-relieved condition, a greater recovery in hardness was observed as the annealing temperature increased from 1400 to 1600°F.

C. THERMAL EXPOSURE

Tensile specimens of nine bimetal composite combinations were thermally exposed for 1600 hours at 1500°F. After exposure the specimens were bowed, with the refractory material on the outside. A discussion of the observed bowing is presented in the next section of this report. All the specimens appeared sound with the exception of the Ta/Inconel 600 specimen which was almost entirely delaminated. At the request of the NASA contracting officer, five of these specimens (Ta/321, FS-85/321, Cb/Inconel 600, Cb-1Zr/Inconel 600, and the delaminated Ta/Inconel 600) were tested in tension at room temperature without being first straightened. Dye penetrant inspection of the four apparently sound specimens prior to testing revealed no indications of delamination. These test results and the room temperature results obtained on the composites in the as-received condition are reviewed in Table 7. The Ta/Inconel 600 composite was delaminated along the entire gage length prior to fracture although fracture occurred simultaneously in both components at the same point. The remaining three composites (Ta/321, Cb/Inconel 600, and Cb-1Zr/Inconel 600) remained intact during testing and the interface delaminated back from the fracture only approximately 1/8 inch. There was a general reduction in the strength level concomitant with the increase in

*The bulk hardness value was determined 20 mils from the interface and is assumed to represent changes caused by shock hardening during bonding and subsequent recovery thereof.

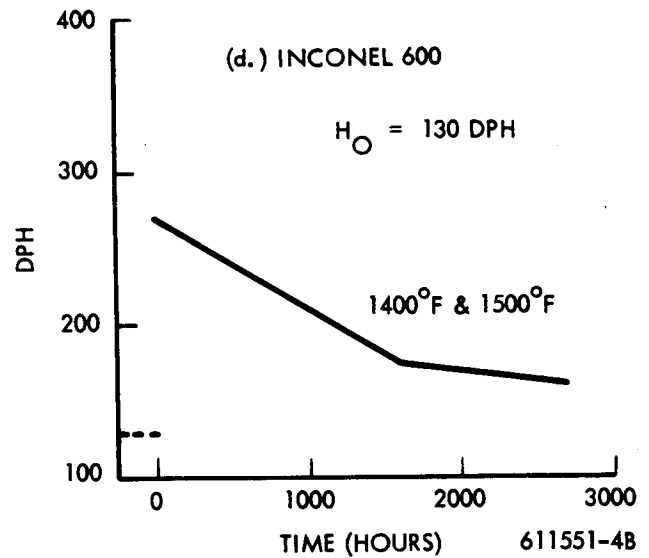
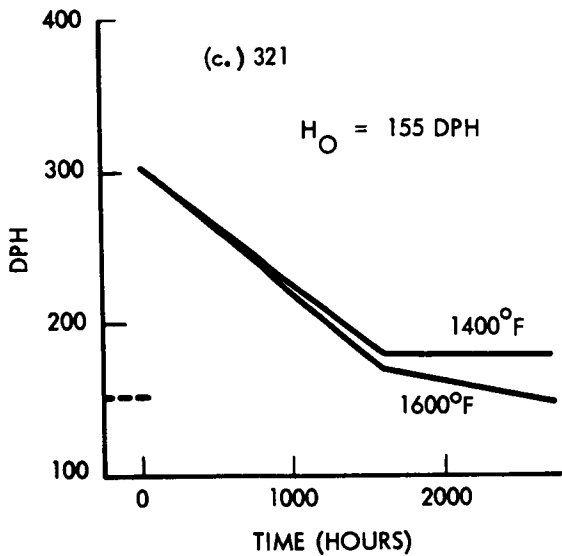
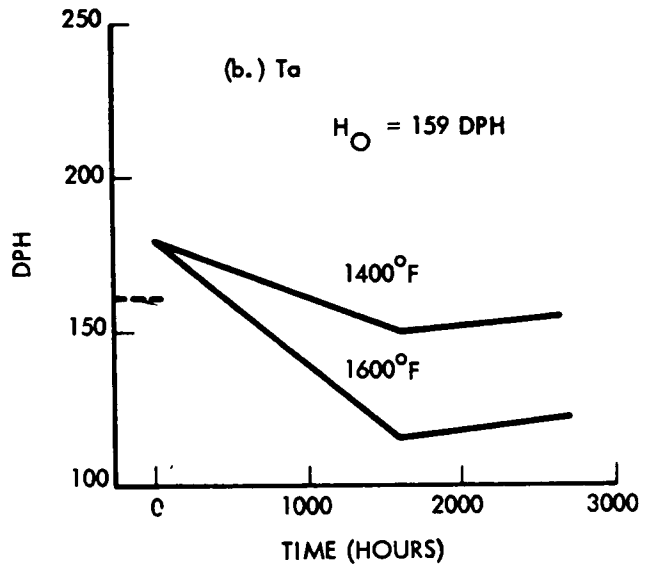
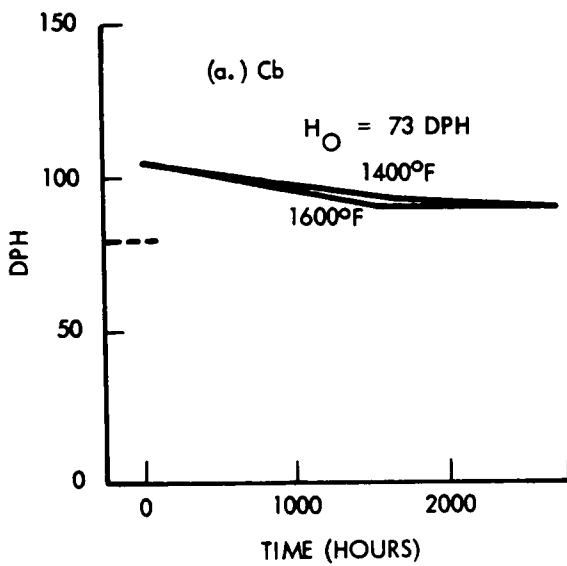


FIGURE 11 - Hardness Change in Refractory and Austenitic Components after Annealing for Specified Time. (H_0 is Hardness of Material Prior to Explosive Bonding).

TABLE 7 - Room Temperature Tensile Test Data on Refractory/Austenitic/Bimetal Composites As-Bonded and After Thermal Exposure of 1600 Hours at 1500°F

Composition	0.2% Yield Strength (ksi)	Ultimate Strength (ksi)	Elongation (%)			Red. in Area (%)			Condition (a)
			Refractory	Total	Austenitic	Refractory	Austenitic	Condition (b)	
Ta/321	43.7	77.3	59.4		61.6	83.3	63.1	ATE ^(b)	
	92.0	96.6		20.0		62.1	56.8	AB	
	90.1	94.8		31.0		59.5	55.5	AB	
FS-85/321	52.4	84.6	53.5		55.1	65.9	66.3	ATE ^(c)	
	98.6	102.1		26.0		47.7	56.9	AB	
	97.5	101.4		28.0		40.0	56.2	AB	
Cb/Inc. 600	26.5	65.5	52.5		52.0	65.6	54.2	ATE ^(b)	
	75.1	81.0		24.0		80.9	59.2	AB	
	73.2	80.9		30.0		81.1	56.1	AB	
Cb-1Zr/Inc. 600	28.9	69.8	48.0		48.0	78.0	54.3	ATE ^(b)	
	82.8	90.9		22.0		61.2	55.0	AB	
	81.8	90.7		22.0		60.3	56.3	AB	
Ta/Inc. 600	18.5	52.2	12.0		50.0	82.2	51.0	ATE ^(d)	
	90.3	94.0		21.0		63.8	68.7	AB	
	89.3	93.7		21.0		66.7	52.8	AB	

(a) ATE - As-Thermally Exposed

AB - As-Bonded

(b) Delaminated 1/8" near fracture.

(c) Delaminated along entire gage length during test.

(d) Delaminated prior to test.

ductility. The decrease in strength of the composites can be attributed primarily to the recovery of the austenitic components. During explosive bonding, the higher rate of work hardening austenitic stainless steels exhibited a significant increase in bulk hardness while the refractory metal components exhibited only a minor increase⁽⁵⁾. As shown earlier, the austenitic components has essentially recovered the annealed strength properties after 1600 hours at 1400°F.

D. THERMAL CYCLING

Several minor alterations were made to the thermal cycling apparatus to reduce the time required for cooling the specimens (from 1350°F to 600°F) from the 90 seconds originally required to 30 seconds. These alterations consisted of reducing the mass of the molybdenum restraining fixture and repositioning the helium cooling jets. An oxygen gage, used to monitor the quality of the helium gas, was also added to the system to complete the instrumentation. Photographs of the restraining fixture and of the system are shown in Figures 12 and 13.

Checkout of the apparatus was completed and two 1 inch x 8 inch specimens of each of the nine selected composites in the as-received condition were thermally cycled, 20 times each. Each cycle, performed on three specimens simultaneously, consisted of heating from 600°F to 1350°F in 5 minutes, holding at temperature for 15 minutes, and cooling to 600°F in approximately 30 seconds. Further details of the testing procedure and conditions are given in the Second Quarterly Progress Report⁽⁵⁾. The cycles were extremely uniform within each run and from run to run. Time to cool from 1350°F to 600°F varied from 35 to 45 seconds, with a maximum variation of 5 seconds for any one run. The axial temperature distribution over the 8 inch long specimens at temperature was less than 30°F.

Upon release from the restraining fixture, the cycled specimens invariably bowed, with the refractory material to the outside. The amount of bow, as defined by Figure 14, was determined and the data are recorded in Table 8. Empirically the amount of bow appears to be dependent upon the strength of the refractory metal component (i. e., the weaker the refractory material, the less the amount of bow). The composition of the austenitic component

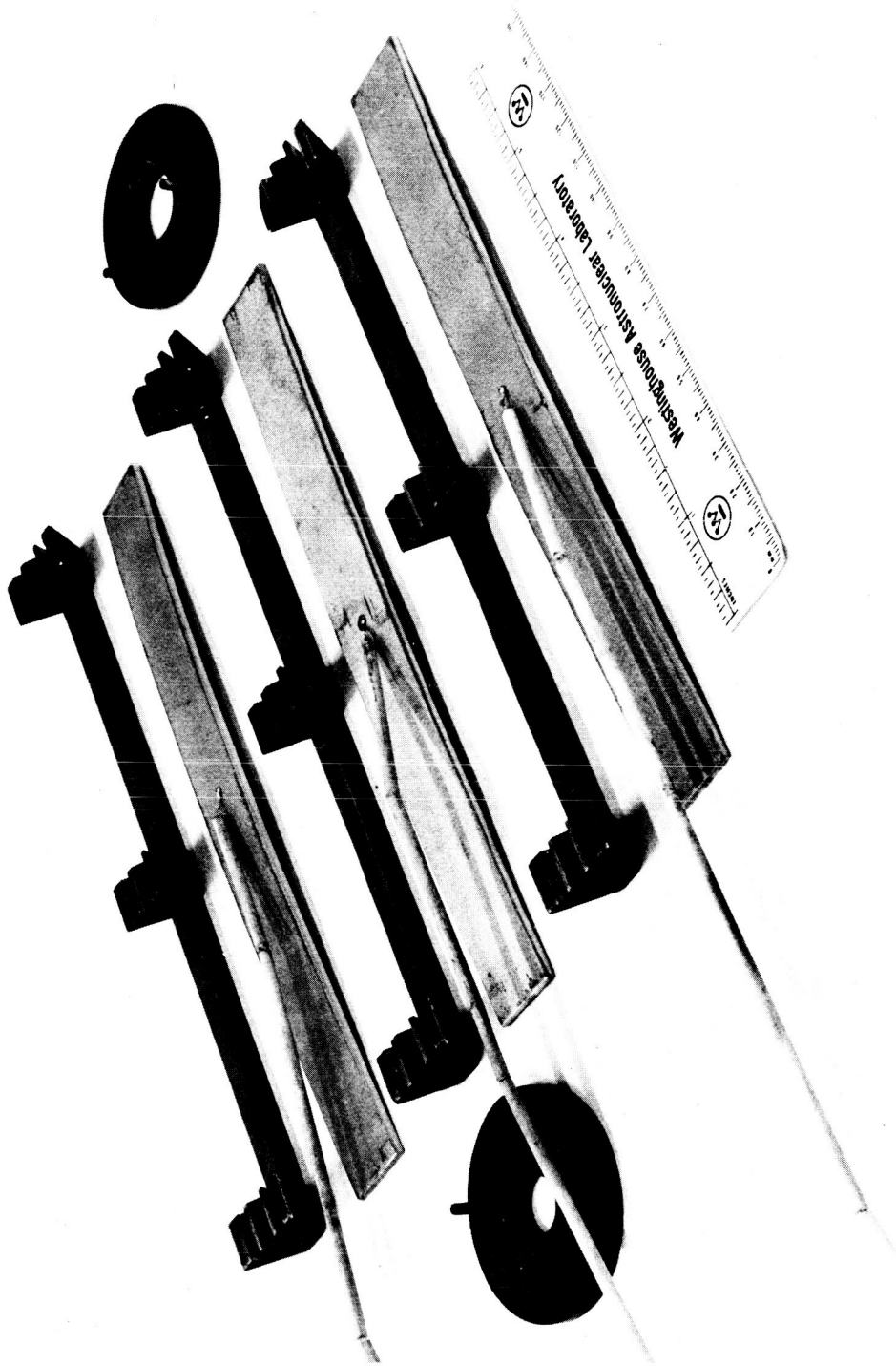


FIGURE 12 - Thermal Cycle Specimens and Restraint Fixture Prior to Assembly

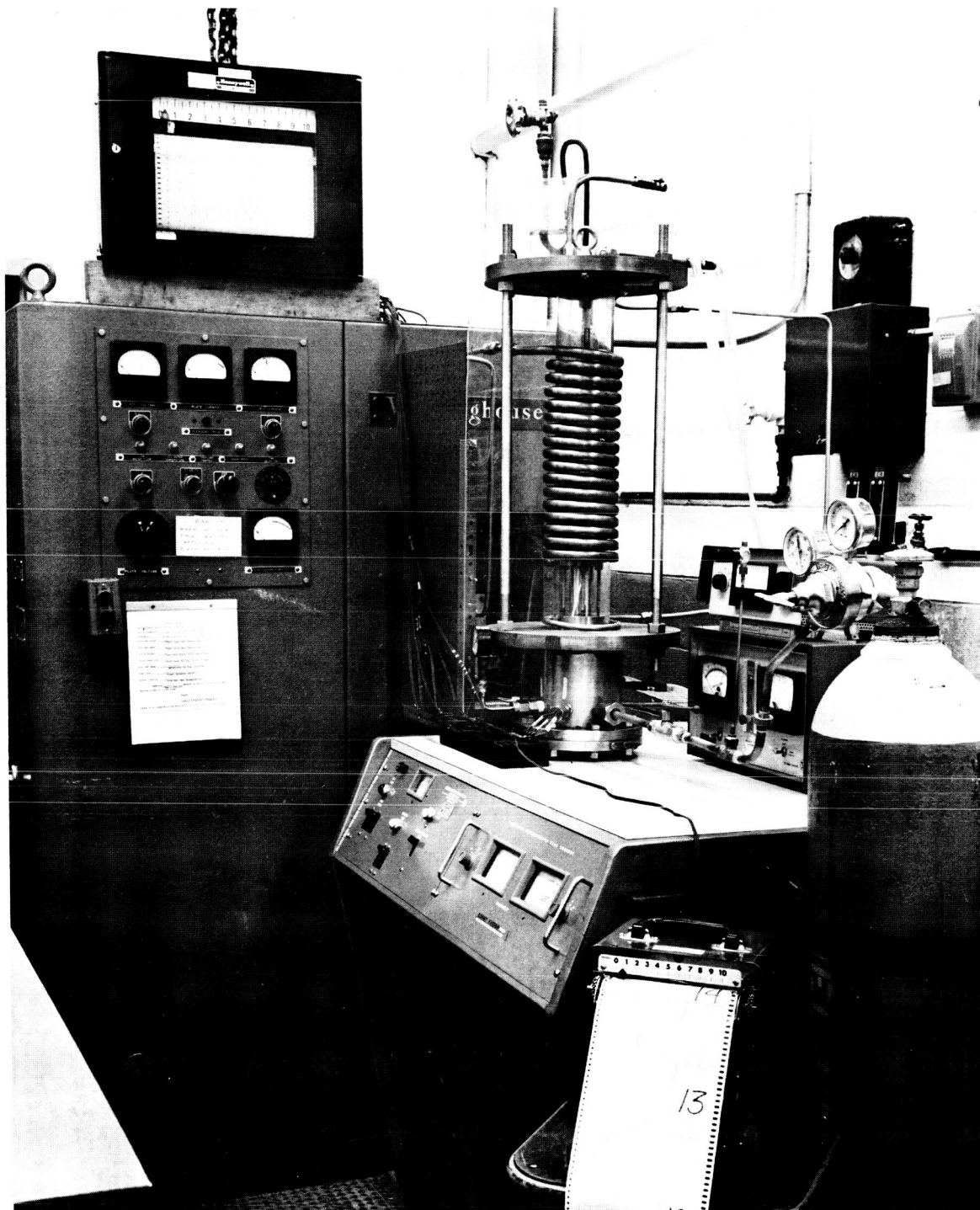
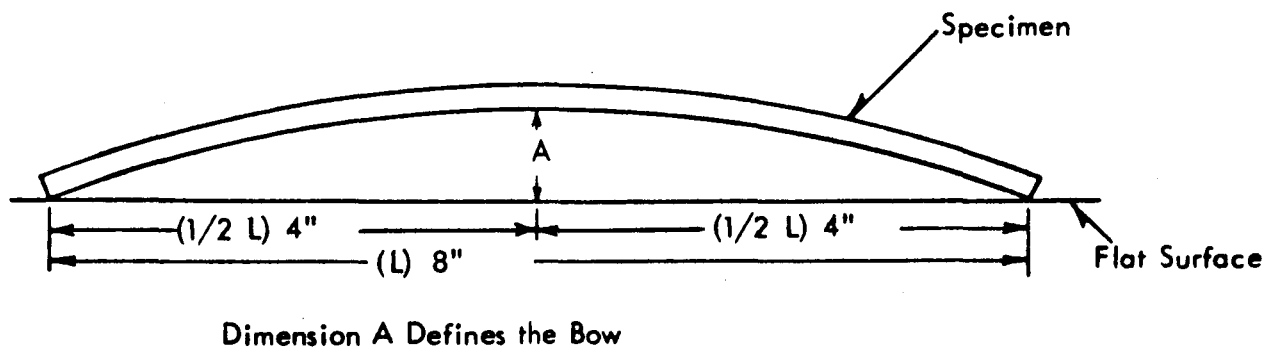


FIGURE 13 - Thermal Cycling Test Rig



NOTE: Refractory metal portion on outside radius of curvature.

FIGURE 14 - Schematic View of Thermally Cycled Strip Showing Direction of Bow

TABLE 8 - Amount of Bow^(a) of Bimetal Composites Resulting from Thermal Cycling

Composition	Specimen No.	Bow ^(a) (inches)
Cb/347	10-3	0.09
Cb/347	10-4	0.10
Cb/321	2-3	0.13
Cb/321	2-4	0.12
Cb/Inc. 600	5-3	0.12
Cb/Inc. 600	5-4	0.13
Cb-1Zr/Inc. 600	20-3	0.25
Cb-1Zr/Inc. 600	20-4	0.23
Cb-1Zr/347	8-3	0.25
Cb-1Zr/347	8-4	0.25
Ta/347	13-3	0.33
Ta/347	13-4	0.34
Ta/Inc. 600	12A-3	0.34
Ta/Inc. 600	12A-4	0.34
Ta/321	15-3	0.37
Ta/321	15-4	0.38
FS-85/321	11-7	0.57
FS-85/321	12-1	0.57

(a) Bow is defined by Figure 14.

of the composite did not have any apparent effect on the amount of bow. An analysis of the stresses occurring during the thermal cycling shows that it is indeed the strength of the refractory component (at 1350°F) of a composite that determines the amount of bow. During heat-up, the greater expansion coefficients of the austenitic materials (i. e. , about 10×10^{-6} in/in/°F versus about 4×10^{-6} in/in/°F for the refractory materials) tend to bow the specimens with the austenitic material to the outside. The austenitic component plastically deforms in compression during the time the specimens are at temperature because the restraint fixture prevents any bending. The amount of this plastic deformation is proportional to the strength of the refractory material. During cooldown, the greater thermal contraction of the austenitic material reverses the stresses tending to bow the specimens in the opposite direction. It is this state of stress which accounts for the observed bow when the specimens are released from the fixture. No delaminating of the cycled specimens was observed during visual examination. (However, a few very minor defects which were not present prior to testing were observed by dye penetrant inspection.) These results are listed in Table 9.

Ultrasonic inspection for further indications of interface defects was performed on the cycled specimens. The results of the ultrasonic resonance test (Vidigage), previously used to inspect the as-received material⁽⁶⁾, indicated that much unbonding had occurred during the severe thermal cycling. However, these results were not considered conclusive as specimens which were reported to have interface separations were sound when sectioned and examined metallographically. The cycled specimens, as well as several other pieces of bimetal composites known to have defective interfaces, were again ultrasonically inspected, this time using a pulse echo technique. A type UM 715 Sperry Reflectoscope with a 20 MHz 3/8 inch diameter focused lithium sulfate transducer driven at 10 MHz was employed. Each strip was placed under the transducer in an immersion tank with the 0.030 inch refractory metal side next to the transducer in order to provide the greatest displacement in the ultrasonic reflection pattern in the presence of any unbonded area. The water distance between the transducer and each composite specimen was adjusted to produce the maximum successive

**TABLE 9 - Results of Dye Penetrant Inspection of As-Received Plus
As-Thermally Cycled Composite Specimens**

Composition	Specimen No.	Dye Penetrant Indications
Cb/321	2-3	1/4" Defect (1 end)
Cb/321	2-4	None
Cb/Inc. 600	5-3	None
Cb/Inc. 600	5-4	None
Cb-1Zr/347	8-3	1/8" Defect (2" from end)
Cb-1Zr/347	8-4	1/8" Defects (2" from end - both sides)
Cb/347	10-3 ^(a)	1/2" Defect (1 end)
Cb/347	10-4 ^(a)	1/8" Defect (1 end)
FS-85/321	11-7	None
FS-85/321	12-1	1/8" Defect (1-1/2" from end)
Ta/Inc. 600	12A-3	None
Ta/Inc. 600	12A-4	None
Ta/347	13-3	1/4" Defect (both ends)
Ta/347	13-4	None
Ta/321	15-3	None
Ta/321	15-4	1/8" Defect (1 end)
Cb-1Zr/Inc. 600	20-3	None
Cb-1Zr/Inc. 600	20-4	1/8" Defect (1 end)

(a) Austenitic material cooled by helium gas.

reflection pattern through the total 0.090 inch specimen thickness. Testing was performed by traversing each specimen over its entire length at 1/4 inch intervals. The differences in indications of a sound bond and an unsound bond are illustrated in Figure 15. The horizontal distance between peaks in Figure 15a represents the total thickness, while the much smaller distance between peaks in the more erratic decay curve of Figure 15b represents the 30 mil thick refractory component only. Metallographic examination of the pieces of bimetal composites known to have unbonded areas verified the presence or absence of bonding as indicated by the pulse echo technique. No unbonded areas were indicated in the thermally cycled strips. Thus it is concluded that all of the cycled specimens capably withstood the repeated severe thermal cycles, and that the few edge defects indicated by the dye penetrant inspection were shallow.

These specimens will now be roll straightened and re-inspected for interface separation, prior to having tensile and stress-rupture specimens machined from them.

E. CREEP RUPTURE

Creep rupture testing at 1350°F of the as-explosively bonded composites was initiated during this period. The test results obtained are listed in Table 10. None of the composites tested ruptured during the test, thus time to 1% elongation was used for comparison with rupture data for type 321 and type 347 stainless steel (see Figure 16). From the data plotted in Figure 16, it is apparent that the composite is stronger than the stainless steel component. However creep is strongly affected by prior thermal-mechanical history as evidenced by the lower rupture strength of the cold worked 347 stainless steel with respect to fully annealed material as illustrated in Figure 16.

TABLE 10 - 1350°F Creep Rupture Properties of Refractory Austenitic Bimetal Composites

Composite	Stress (psi)	Test Duration (hours)	Total Elongation	Time to 1% Strain
Ta/321	14,000	1,110	1.15	870
Cb-1Zr/347	11,000	1,007	0.17	---
Cb/321	10,000	657	3.54	312

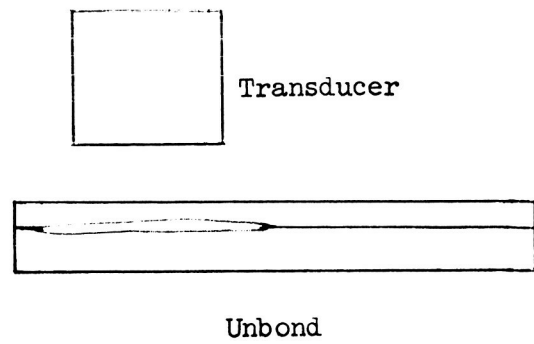
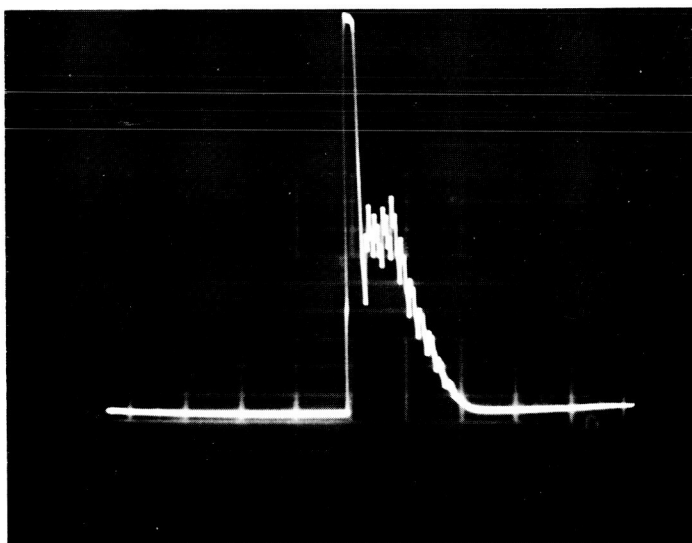
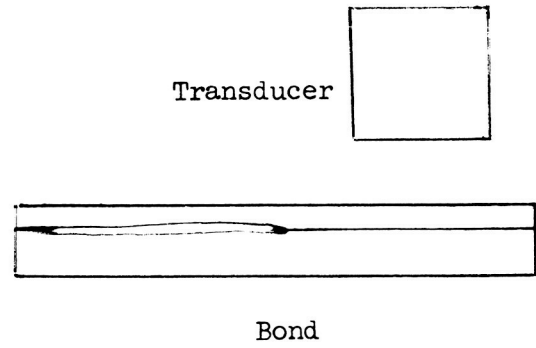
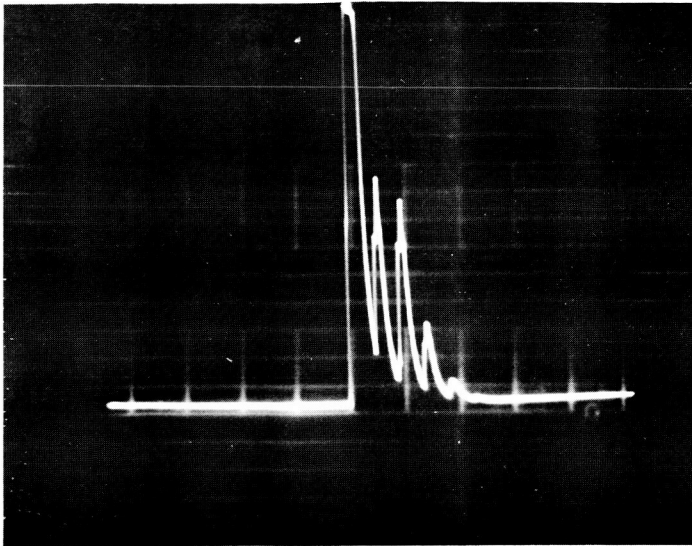


FIGURE 15 - Appearance of Indications of Bonded and Unbonded Bimetal Composites Using Pulse Echo Ultrasonic Technique

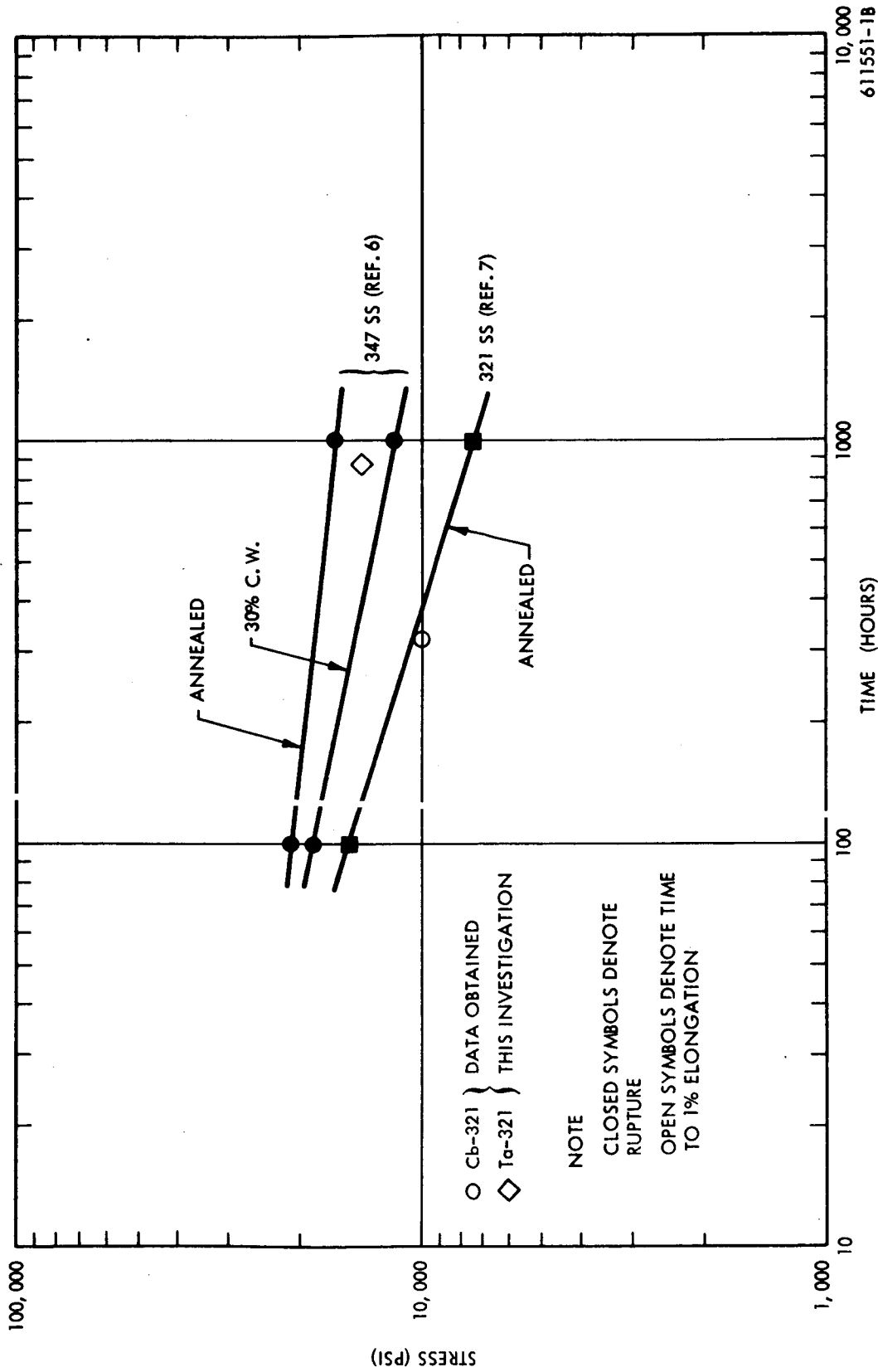


FIGURE 16 - Creep and Creep Rupture Data for Austenitic Stainless Steel and Austenitic/Refractory Bimetal Composites at 1350°F

The metallurgical condition of the as-bonded bimetal composites varies across the thickness with the area near the interface highly deformed and the bulk hardness of each component significantly increased by the shock loading during bonding⁽⁵⁾. This bulk hardness increase is indicative of a high percentage of cold work. One would expect therefore a significant decrease in the 321 and 347 rupture strength. The fact that this is not evidenced shows that the creep strength of the composite has been significantly increased by the refractory metal component.

The test specimens have a 1 inch gage length with a 0.250 inch reduced section. Creep tests are being conducted under conditions of ultra-high vacuum ($<1 \times 10^{-8}$ torr) in a dead weight loaded system⁽⁶⁾. Distortion of the specimen during heating to test temperature necessitates application of the load prior to the start of heat-up. Otherwise, the specimen cannot be viewed optically and strain measurement is not possible. After establishment of the creep-rupture behavior of the as-bonded material, several selected thermally exposed and thermally cycled specimens will be tested.

After test, the bimetal creep specimens are bowed with the refractory metal component to the outside of the bow. The reasons are essentially the same as discussed previously for the thermally cycled specimens.

III. FUTURE WORK

During the next period, the following will be accomplished:

1. The diffusion annealing work including data analysis will be completed.
2. The nine selected diffusion annealed specimens will be prepared for electron beam microprobe analyses.
3. Evaluation of the thermally cycled as-received bimetal strips will be completed.

4. The 1500°F, 1600 hour thermal exposure run will be completed and the specimens will be inspected, straightened, and re-inspected.

5. The as-thermally exposed tensile specimens will be tested and the 1 inch x 8 inch strips will be thermally cycled, inspected, and tested.

6. Stress-rupture testing of bimetal composites in the as-received and thermally exposed (1500°F, 1600 hours) conditions will be continued.

IV. REFERENCES

1. A. V. Manzione, F. J. Heugel, and D. E. Fornwalt, Observations Concerning the Interdiffusion of Cb-1Zr Alloy with Type 316 Stainless Steel, CNLM-5232, 1963.
2. H. S. Goldschmidt, Research 10, 289, 1957.
3. L. S. Birks and R. E. Seebold, J. of Nucl. Mat. 3, 249, 1961.
4. P. B. Ferry and J. P. Page, "Metallurgical Study and Niobium/Type 316 Stainless Steel Duplex Tubing", NAA-SR-11191, January 5, 1966.
5. R. W. Buckman, Jr. and J. L. Godshall, "Evaluation of Refractory/Austenitic Bimetal Combinations", Second Quarterly Progress Report, WANL-PR(EE)-002, Contract NAS 3-7634.
6. J. L. Godshall and R. W. Buckman, Jr., "Evaluation of Refractory/Austenitic Bimetal Combinations", First Quarterly Progress Report, WANL-PR(EE)-001, Contract NAS 3-7634.
7. N. Grant, et al, "Creep Rupture Properties of Cold Worked Type 347 Stainless Steel" Trans. ASM, Vol 48, 1956, p. 446.
8. W. Simmons and H. Cross, "The Elevated Temperature Properties of Stainless Steel" ASTM-STP-124.

Metallographic Preparation of Refractory/Austenitic Bimetal Composites

The method for metallographically preparing specimens of refractory/austenitic bimetal composites is as follows:

Mechanical Polishing: All of the bimetal composite specimens, regardless of their compositions, are polished in the same manner. Initially the specimens are mounted in bakelite and ground on 120 through 600 grit silicon carbide papers. The scratches from the last paper are then removed by polishing with 30, 15, and 6 micron diamond abrasives for short times on Metcloth, using a few drops of lapping oil as a lubricant. The mechanical polishing is then continued on Microcloth charged with a thick, hot slurry of Linde B alumina abrasive and water. * This process, used for 6 minutes with heavy pressure and for 1 minute with light pressure, polishes down below the scratches on the austenitic materials, while leaving only slight scratching on the refractory materials. To complete the polish on the refractory materials, the specimens are finally polished for 1 hour in a Syntron using a very thin slurry of Linde B and water.

Etching: Etching of the different austenitic materials of the composite specimens must be done with different etchants, which are listed below. Two etches are listed for Inconel 600 as its etching characteristics appear to be sensitive to differences in its thermal history. However the first etch generally gives the best results and should be tried initially.

321 and 347 Stainless

Etchant - Glyceregia (30 ml HCl 50 ml glycerine, and 15 ml HNO_3)

Procedure - Swab specimen for approximately 1-1/2 minutes. Etch no more than 3 specimens before renewing etchant.

* An appreciable quantity of Linde B is mixed in 250 ml of water and the mixture is heated to boiling just prior to being applied to the Microcloth.

Hastelloy N

Etchant - Nitol (7 ml HNO_3 and 93 ml water)

Procedure - Electrolytically etch specimen for 5 to 10 seconds at 6 volts.

Inconel 600 - Procedure 1

Etchant - Glyceregia (30 ml HCl, 50 ml glycerine, and 15 ml HNO_3)

Procedure - Swab specimen for approximately 1-1/2 minutes

Procedure 2

Etchant - 10 grams of oxalic acid in 90 ml of water

Procedure - Electrolytically etch specimen for 4 to 6 seconds at 6 volts.

Etching procedures are not given for the refractory components of the bimetal composites. The etchants, both chemical and electrolytic, contain hydrofluoric acid and severely over etch the austenitic components and much of the interdiffusion zones.

DISTRIBUTION LIST

National Aeronautics & Space Administration
Washington, D. C. 20546
Attention: P. R. Miller (RNP)
James J. Lynch (RNP)
George C. Deutsch (RR)
Dr. Fred Schulman (RNP)

National Aeronautics & Space Administration
Scientific & Technical Information Facility
P. O. Box 5700
Bethesda, Maryland 20014
2 copies + 2 reproducibles

National Aeronautics & Space Administration
Ames Research Center
Moffett Field, California 94035
Attention: Librarian

National Aeronautics & Space Administration
Goddard Space Flight Center
Greenbelt, Maryland 20771
Attention: Librarian

National Aeronautics & Space Administration
Langley Research Center
Hampton, Virginia 23365
Attention: Librarian

National Aeronautics & Space Administration
Manned Spacecraft Center
Houston, Texas 77001
Attention: Librarian

National Aeronautics & Space Administration
George C. Marshall Space Flight Center
Huntsville, Alabama 35812
Attention: Librarian

National Aeronautics & Space Administration
Jet Propulsion Laboratory
4800 Oak Grove Drive
Pasadena, California 91103
Attention: Librarian

National Aeronautics & Space Administration
Lewis Research Center
21000 Brookpark Road
Cleveland, Ohio 44135
Attention: Librarian
Dr. Bernard Lubarsky 500-201
Roger Mather 500-309
H. O. Slone 500-201
G. M. Ault 105-1
P. L. Stone 500-201 2 copies
G. M. Thur 500-201
John E. Dilley 500-309
John Weber 3-19
T. A. Moss 500-309
Dr. Louis Rosenblum 106-1
C. A. Barrett 106-1
Report Control Office 5-5

National Aeronautics & Space Administration
Western Operations Office
150 Pico Boulevard
Santa Monica, California 90406
Attention: Mr. John Keeler

National Aeronautics & Space Administration
Azusa Field Office
P. O. Box 754
Azusa, California 91703
Attention: Fred Herrmann

National Bureau of Standards
Washington 25, D. C.
Attention: Librarian

AFSC
Aeronautical Systems Division
Wright-Patterson Air Force Base, Ohio 45433
Attention: Charles Armbruster (ASRPP-10)
T. Cooper
Librarian



Army Ordnance Frankford Arsenal
Bridesburg Station
Philadelphia, Pennsylvania 19137
Attention: Librarian

U. S. Atomic Energy Commission
Germantown, Maryland 20767
Attention: H. Rothen, SNAP 50/SPUR
Project Office
Maj. Gordon Dicker, SNAP
50/SPUR Project Office

U. S. Atomic Energy Commission
Technical Information Service Extension
P. O. Box 62
Oak Ridge, Tennessee 37831

U. S. Atomic Energy Commission
Washington, D. C. 20545
Attention: M. J. Whitman

Argonne National Laboratory
9700 South Cass Avenue
Argonne, Illinois 60440
Attention: Librarian

Brookhaven National Laboratory
Upton, Long Island, New York 11973
Attention: Librarian
Dr. D. H. Gurinsky
Dr. J. R. Weeks

Oak Ridge National Laboratory
Oak Ridge, Tennessee 37831
Attention: Mr. J. Devan
Mr. A. Taboada
Mr. H. W. Savage
Librarian

Office of Naval Research
Power Division
Washington, D. C. 20360
Attention: Librarian

Bureau of Weapons
Research and Engineering
Materials Division
Washington 25, D. C.
Attention: Librarian

U. S. Naval Research Laboratory
Washington, D. C. 20390
Attention: Librarian

Aerojet-General Nucleonics
P. O. Box 77
San Ramon, California 94583
Attention: B. E. Farwell

Aerojet-General Corporation
Von Karman Center
Azusa, California 91703
Attention: M. Parkman
R. S. Carey
H. Derow

AiResearch Manufacturing Company
Division of the Garrett Corporation
Sky Harbor Airport
402 S. 36th Street
Phoenix, Arizona 85034
Attention: Librarian
E. A. Kovacevich

AiResearch Manufacturing Company
Division of The Garrett Corporation
9851-9951 Sepulveda Boulevard
Los Angeles, California 90009
Attention: Librarian

IIT Research Institute
10 W. 35th Street
Chicago, Illinois 60616
Attention: Librarian

Babcock & Wilcox Company
Research Center
Alliance, Ohio
Attention: Librarian

North American Aviation, Inc.
Atomics International Division
8900 DeSoto Avenue
Canoga Park, California 91304
Attention: Librarian
J. P. Page
P. B. Ferry

AVCO
Research & Advanced Development Dept.
201 Lowell Street
Wilmington, Massachusetts
Attention: Librarian

Battelle Memorial Institute
505 King Avenue
Columbus, Ohio
Attention: Librarian

DuPont de Nemours Co.
Eastern Lab
Gibbstown, New Jersey
Attention: A. Holtzman
A. Popoff
J. Ransome
K. Mietzner

Electro-Optical Systems, Inc.
Advanced Power Systems Division
Pasadena, California 91107
Attention: Librarian

Fansteel Metallurgical Corporation
North Chicago, Illinois
Attention: Librarian

Philco Corporation
Aeronutronics
Newport Beach, California 92663
Attention: Librarian

General Atomic Division of General
Dynamics Corp, John Jay Hopkins Lab.
P. O. Box 608, San Diego, California 92112
Attention: Librarian

General Electric Company
Flight Propulsion Laboratory Department
Cincinnati, Ohio 45215
Attention: Librarian

General Electric Company
Missile & Space Vehicle Department
3198 Chestnut Street
Philadelphia, Pennsylvania 19104
Attention: Librarian

General Electric Company
Missile & Space Division
Cincinnati, Ohio 45215
Attention: Librarian

General Electric Company
Vallecitos Atomic Laboratory
Pleasanton, California 94566
Attention: Librarian

General Electric Company
Evendale, Ohio 45215
FPD Technical Information Center
Bldg. 100, Mail Drop F-22

General Dynamics/Fort Worth
P. O. Box 748
Fort Worth, Texas
Attention: Librarian

General Motors Corporation
Allison Division
Indianapolis, Indiana 46206
Attention: Librarian

Hamilton Standard
Division of United Aircraft Corporation
Windsor Locks, Connecticut
Attention: Librarian

Hughes Aircraft Company
Engineering Division
Culver City, California
Attention: Librarian



**Astronuclear
Laboratory**

Lockheed Missiles & Space Division
Lockheed Aircraft Corporation
Sunnyvale, California
Attention: Librarian

The Martin Company
Nuclear Division
P. O. Box 5042
Baltimore, Maryland 21203
Attention: Librarian

Martin Marietta Corporation
Metals Technology Laboratory
Wheeling, Illinois

Materials Research Corporation
Orangeburg, New York
Attention: Librarian

McDonnell Aircraft
St. Louis, Missouri
Attention: Librarian

MSA Research Corporation
Callery, Pennsylvania 16024
Attention: Librarian

National Research Corporation
70 Memorial Drive
Cambridge, 42, Massachusetts
Attention: Librarian

North American Aviation
Los Angeles Division
Los Angeles, California 90009
Attention: Librarian

United Aircraft Corporation
Pratt & Whitney Aircraft Division
400 Main Street
East Hartford, Connecticut 06108
Attention: Librarian

Republic Aviation Corporation
Farmingdale, Long Island, New York 11735
Attention: Librarian

Solar
2200 Pacific Highway
San Diego, California 92112
Attention: Librarian

Southwest Research Institute
8500 Culebra Road
San Antonio 6, Texas
Attention: Librarian

Superior Tube Company
Norristown, Pennsylvania
Attention: L. Shaheen

TRW, Inc.
23555 Euclid Avenue
Cleveland, Ohio 44117
Attention: Mr. J. J. Owens
Mr. E. J. Vargo
Librarian

Union Carbide Corporation
Stellite Division
P. O. Box 746
Kokomo, Indiana 46901
Attention: Librarian
Technology Department

University of Michigan
Ann Arbor, Michigan 48103
Attention: Dr. R. E. Balshiser

Wah Chang Corporation
Albany, Oregon
Attention: Librarian

Volverine Tube Division
Calcumet and Hecla, Inc.
17200 Southfield Road
Allen Park, Michigan
Attention: Mr. Eugene F. Hill